Context-Aware Decentralized Invariant Signaling for Opportunistic Communications

Jordi Borràs and Gregori Vázquez

Abstract

A novel scenario-adapted distributed signaling technique in the context of opportunistic communications is presented in this work. Each opportunistic user acquires locally sampled observations from the wireless environment to determine the occupied and available degrees-of-freedom (DoF). Due to sensing errors and locality of observations, a performance loss and inter-system interference arise from subspace uncertainties. Yet, we show that addressing the problem as a total least-squares (TLS) optimization, signaling patterns robust to subspace uncertainties can be designed. Furthermore, given the equivalence of minimum norm and TLS, the latter exhibits the interesting properties of linear predictors. Specifically, the rotationally invariance property is of paramount importance to guarantee the detectability by neighboring nodes. Albeit these advantages, end-to-end subspace uncertainties yield a performance loss that compromises both detectability and wireless environment's performance. To combat the latter, we tackle the distributed identification of the active subspace with and without side information about neighboring nodes' subspaces. An extensive simulation analysis highlights the performance of distributed concurrency schemes to achieve subspace agreement.

Index Terms

Opportunistic communications, distributed networks, decentralized signaling, total least-squares, invariance, sensing uncertainties.

The research leading to this work has been funded by the Spanish Ministry of Science, Innovation and Universities under the project WINTER: TEC2016-76409-C2-1-R (AEI/FEDER, UE) and fellowship FPI BES-2017-080071, and by the Catalan Government (AGAUR) through the grant 2017 SGR 578.

The authors are with the Department of Signal Theory and Communications of the Technical University of Catalonia (UPC), Jordi Girona 1-3, Campus Nord Building D5, 08034 Barcelona, Spain. E-mail: {jordi.borras.pino, gregori.vazquez}@upc.edu

Preliminary results have been presented at 2019 IEEE International Conference on Communications [1] and 2019 IEEE International Workshop on Signal Processing Advances in Wireless Communications [2].

I. Introduction

The concept of *Opportunistic Communications* [3] refers to robustly and efficiently exploiting the available resources in a wireless network and adapting information transmission to the network state. The research in opportunistic communications has been basically centered in enhancing the spectral efficiency by smartly exploiting spectral resources. Therefore, this communication format can be seen as an enabler for providing high data-rates in congested networks. Furthermore, opportunistic communications also enable data transmission in *infrastructureless* networks, which means that inefficient backbone communication can be avoided.

Opportunistic communications were firstly studied in [4], under the concept of opportunistic beamforming, as a multiuser scheduling scheme in point-to-point ergodic fading channels. The strategy in [4] did not require full channel state information (CSI) at transmitter side, but only the channel quality. Hence, the transmission only would take place when we have a good opportunity, that is when we enjoy favorable channel conditions, to do so. Similarly, this idea is also considered to enhance the agility and flexibility of wireless networks by permitting the coexistence of users with different priorities in view of the use of radio resources. We may refer to techniques such as cognitive radio [5] (specially the interweave paradigm [6]), heterogeneous networks [7], device-to-device communications [8] and dynamic spectrum access [9].

In order to achieve their main goals, opportunistic nodes need to be aware of the wireless network state. To do so, they require specific techniques encompassed in the family of sensing techniques. Generally speaking, *degrees-of-freedom (DoF) sensing* permits opportunistic users to determine occupied and available DoF. Therefore, they can use this information to appropriately modulate the information.

A huge number of contributions on sensing techniques [10] is available in the literature. Therefore, throughout this work we assume that sensing has already been performed, and we focus our research on opportunistic transmission schemes. Nevertheless, the study of the impact of sensing errors will be an important aspect of this contribution.

A. Prior Work

The most powerful idea in the context of signaling for opportunistic communications is the so-called *null-space* opportunistic transmission [11]. This concept is based on the exploitation of the orthogonal subspace to those DoF sensed as occupied by opportunistic users. The orthogonal

subspace, also known as *noise subspace*, contains single- or multi-channel DoF detected as available, whereas the so-called *signal subspace* encompasses those occupied DoF.

It is worth noticing that it is not strictly necessary the exploitation of the noise subspace to avoid or minimize the interference to the signal subspace. In this sense, opportunistic transmission can be addressed in both time and frequency domains. Regarding to the former, an interesting idea relies on exploiting the cyclic prefix (CP) of the orthogonal frequency-division multiplexing (OFDM) transmissions of primary users [12], known as Vandermonde-subspace Frequency-Division Multiplexing (VFDM). Albeit it was initially developed for single-user scenarios, the multi-user approach has been recently studied [13], [14]. Recalling the frequency domain, the authors exploited in [15] the excess of bandwidth of communication channels with roll-off to jointly transmit and monitor wireless environment's activity. Thus, when available DoF are detected as occupied, opportunistic users stop using them to avoid inter-system interference. Even though the use of these non-orthogonal techniques allows opportunistic transmission, noise enhancement or inter-system interference may appear when opportunistic users are not synchronized with the wireless environment. Thus, herein we will focus our discussion on the aforementioned noise subspace approaches.

Regarding to the exploitation of multi-channel DoF, several works can be found in multi-antenna scenarios. In this case, opportunistic signals are precoded such that throughput is maximized and they are as much orthogonal as possible to the interference channel matrices. One critical issue is the knowledge of these matrices. In the literature, we may found three different approaches: instantaneous CSI [16], imperfect CSI (cf. [17–19]), and statistical CSI [11], [20], [21] (which relies on second-order statistics estimation). As a final comment, multi-channel VFDM was explored in [22].

Even though the waveform design problem for opportunistic communications has been widely studied, it is still an opened issue, specially in the sense of coexistence of several technologies in heterogeneous environments. In this sense, the waveform design for system coexistence or the use of improper Gaussian signaling are studied in [23] and [24], respectively. In view of the lack of radio resources, non-orthogonal multiple access (NOMA) techniques for cognitive communications are surveyed in [25].

B. Contributions

The major contribution of this work is presented in Sec. III. We address the design of *invariants* in distributed communications. In this sense, we introduce a novel scenario-adapted shaping filter design scheme for opportunistic communications. Thanks to the existence of invariances, the proposed signaling can be exploited in uncoordinated decentralized heterogeneous networks. As discussed in Sec. II, the proposed technique can be used either for opportunistic data transmission and also for achieving pilot orthogonality, regardless the possible correlation of pilot pseudo-noise (PN) sequences. Finally, we address subspace concurrency algorithms at both system ends to improve the performance and mitigate inter-system interferences.

C. Notation

In the sequel, boldface lowercase (uppercase) denotes vectors (matrices). $(\cdot)^T$, $(\cdot)^*$ and $(\cdot)^H$ denote the transpose, conjugate, and transpose conjugate (Hermitian) operators. $\mathbf{0}$ denotes the all-zeros vector or matrix of appropriate dimensions. $\mathbf{I}_K$ is the $K \times K$ identity matrix. $\|\cdot\|_0$, $\|\cdot\|_1$, $\|\cdot\|_2$ and $\|\cdot\|_{\mathrm{F}}$ denote the ℓ_0-norm, the ℓ_1-norm, the Euclidean norm, and the Frobenius norm, respectively. $\mathbb{E}\{\cdot\}$ is the mathematical expectation. $\otimes$ stands for the Kronecker product. $\mathrm{diag}[\mathbf{a}]$ refers to a diagonal matrix whose elements are contained in $\mathbf{a}$. A complex Gaussian distribution with mean $\boldsymbol{\mu}$ and covariance $\boldsymbol{\Sigma}$ is denoted as $\mathcal{CN}(\boldsymbol{\mu}, \boldsymbol{\Sigma})$. Uppercase calligraphic letters, e.g. $\mathcal{X}$, denote a subspace or a set. $\dim[\mathcal{X}]$ stands for the dimension of $\mathcal{X}$. $\mathcal{P}(\mathcal{X}; R)$, with $R \leq \dim[\mathcal{X}]$, denotes an R-dimensional portion of $\mathcal{X}$. $\mathrm{span}[\mathbf{X}]$ refers to the subspace spanned by all linear combinations of columns of matrix $\mathbf{X}$.

D. Paper Structure

The remainder of this paper is organized as follows. In Sec. II, we present the signal model and the addressed problem is formally stated. The main result of this work, its formal derivation and the analysis of its properties are presented in Sec. III, IV and V, respectively. The problem of end-to-end subspace miss-match is formulated in Sec. VI. The estimation of active subspace is addressed at receiver and transmitter sides in Sec. VII and VIII, respectively. Numerical results are reported in Sec. IX and the paper is concluded in Sec. X.

II. Signal Model and Problem Formulation

Throughout this work, we consider the scenario depicted in Fig. 1. It is worth noting that two networks can be distinguished in our scenario. Without loss of generality, external network

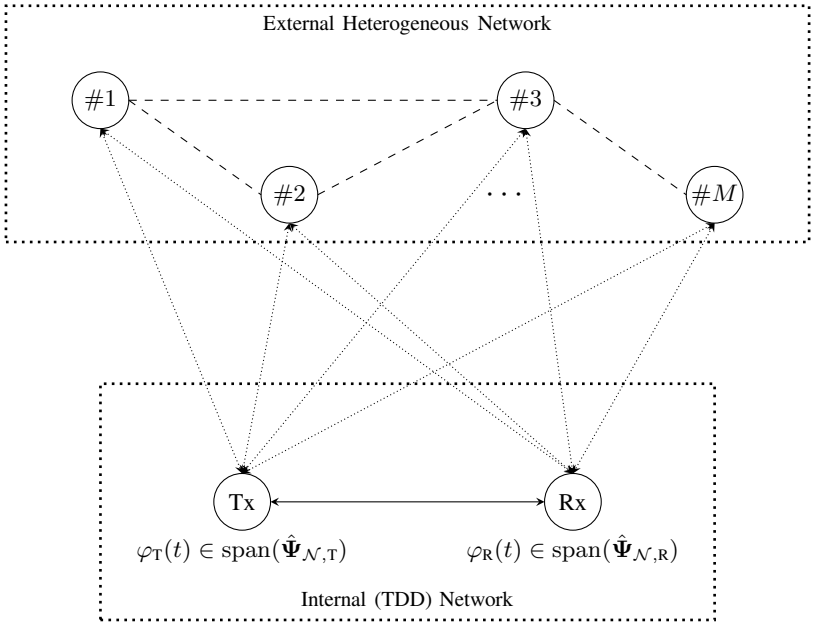

Fig. 1: Context-aware opportunistic communication in a distributed network. Using the interference channels, internal-network users adapt the opportunistic transmissions to avoid inter-system interferences.

is assumed to be an M-user heterogeneous network. With this assumption, several scenarios are contemplated. For instance, external network can be a multi-tier cellular system or an ad-hoc network. In general, these M users use have different modulation and coding schemes. Nonetheless, we consider that they are simultaneously transmitting information exploiting some degrees-of-freedom (DoF). The concept of DoF adopted herein was presented in [26], [27]. That is, the size of the set of complex (real) numbers required to specify any particular class of signals. For signals that are band-limited in $[-W,\ W]$ and time-limited in $[-T/2,\ T/2]$, the number of DoF is upper-bounded by $2WT$ (see the full discussion in [26, Section 8.1]). It is worth noting that there is a slight abuse of notation when describing the concept of external network. Actually, each internal-network user may observe a *different* wireless environment, and hence external network, according to its geographical coordinates. Regarding to the internal network, it is composed of a single-antenna transmitter-receiver pair which wish to opportunistically access the *unused* DoF. To do so, each internal-network user acquires $\ell = 1, \dots L$ locally sampled observations from the external network

$$\mathbf{z}_\ell = \mathbf{s}_\ell + \mathbf{v}_\ell, \tag{1}$$

where $\mathbf{s}_\ell$ is the external-network aggregate signal and $\mathbf{v}_\ell$ is the observation noise distributed as $\mathcal{CN}(\mathbf{0}, \sigma^2\mathbf{I}_N)$. In general, the signals encompassed in $\mathbf{s}_\ell$ have a specific structure, due to the use

of certain modulations or codes. Furthermore, the effect of interference channels is also reflected in these observations. It is worth noting that the length of observations in (1), N, is the number of DoF in our problem. However, only a fraction of N will contain a contribution from external network. Using the set of L observations (1), each internal-network user has to decide if the n-th DoF, ζ_n, is occupied or not. Classically, this problem is tackled as a hypothesis test [10]:

$$\mathcal{H}_0 : \zeta_n \text{ is available} \tag{2a}$$

$$\mathcal{H}_1 : \zeta_n \text{ is occupied} \tag{2b}$$

How this detection problem is solved is out of the scope of this paper. Therefore, the structure of aggregate signals $\mathbf{s}_\ell$ in (1) or the knowledge of interference channels are not required for the purpose of this work. In the literature, we may find several works studying the *sensing* (see, for instance, [10], [28] and references therein). All they are based on *signal detection* theory, with side information about external network or not. As surveyed in [10], the most simple sensing technique is the well-known energy detector. Although it is optimum when external-network transmissions are almost Gaussian signals, its performance is limited in low signal-to-noise ratio (SNR) regimes[1]. Therefore, more sophisticated sensing schemes are based on detecting some features of signals transmitted by external-network users. For instance, sensing mechanisms may exploit the redundancy exhibited by external-network transmissions or their statistical structure. In this sense, some detectors have been developed exploiting second-order statistics (i.e. autocorrelation function) [30], cyclostationarity [31], the structure of covariance matrix of observations [32], or even their spectral structure [33]. However, these mechanisms usually require some side information, as the number of antennas or the coding scheme. In this sense, a technique known as blind detection has been developed. The latter only needs an estimate of the observations' covariance matrix, and its *eigendecomposition*. Examples of relevant blind detectors include, for instance, the maximum-to-minimum eigenvalue ratio test [34] or model order selection [35] based sensing mechanisms [36]. As a final comment on sensing mechanisms, it is important to mention that the sensing task becomes much more challenging as the sensed bandwidth increases. A study on single and multi-frequency wideband sensing can be found in

[1]Basically, this limitation is due to erroneous model assumptions. It is worth noting that energy detection is based on the likelihood ratio, which requires a perfect knowledge of the noise variance to set the appropriate decision threshold. Under worst-case uncertainty, the number of acquired observations to meet the desired performance tends to infinity as the SNR tends to a certain value, known as SNR wall [29].

[37]. The sensing techniques briefly surveyed herein are noncooperative and they do not require (in general) multiple antennas. The reader is referred to, e.g., [38–40] and references therein for further information on cooperative sensing schemes, whereas several multi-antenna approaches can be found in, for instance, [41], [42].

In summary, internal-network users will use the observations in (1) and an arbitrary sensing mechanism to solve the aforementioned hypothesis testing problem. With this information, each internal-network user has to design a shaping filter $\varphi_{\mathrm{i}}(n)$, with $\mathrm{i} = \{\mathrm{T}, \mathrm{R}\}$ referring to transmitter or receiver. Let $a[m]$, T, and S_{R} be a symbol from a given constellation, the symbol period and the received power. Thus, the signal received by internal receiving node $y(n)$ can be written as

$$y(n) = \sum_{m} \sqrt{S_{\mathrm{R}}}\; a[m]\varphi_{\mathrm{T}}(n - mT) + v(n), \tag{3}$$

where $v(n)$ is a circularly-symmetric complex Gaussian noise, i.e. $v(n) \sim \mathcal{CN}(0, \sigma^2)$.

Recalling (3), depending on the meaning of the complex symbols $a[m]$, we can distinguish two different study cases:

(i) If $a[m]$ is an information symbol, the distributed signaling design problem addressed in this work can be seen as an adaptive waveform design problem, a typical problem in opportunistic communications using cognitive radios.

(ii) However, when $a[m]$ is a pseudorandom sequence which spreads the signal energy spectral density, the problem under study becomes a distributed pilot waveform design. Because the number of users in the wireless environment (i.e. taking into account both external and internal networks) can be arbitrarily large, the orthogonality of pilot symbols cannot be guaranteed. Nevertheless, if these pilot sequences are shaped with a context-adapted waveform, pilot contamination can be diminished.

Regardless the potential application, in this work we address the distributed design of shaping filters when internal-network users only take local observations into consideration.

For simplicity of discussion, we present the design of scenario-adapted pulse shaping filters at arbitrary geographical coordinates $\mathbf{r}$. Because in this work we consider a point-to-point opportunistic transmission, $\mathbf{r}$ may be the coordinates of transmitter or receiver. The reported analysis might be then particularized at each internal node. Focusing on the geographical coordinates $\mathbf{r}$, let $D(\mathbf{r})$ be the number of DoF occupied by external-network users. In other words, the ℓ-th sampled external-network aggregate signal belongs to a $D(\mathbf{r})$-dimensional subspace $\mathcal{S}(\mathbf{r})$, i.e. $\mathbf{s}_\ell \in \mathcal{S}(\mathbf{r})$. The latter is typically known as *signal subspace*, denoted by $\mathcal{S}(\mathbf{r})$.

Notice that sampled observations taken by internal-network users consists in N-length vectors. Whether $D(\mathbf{r}) < N$, $K(\mathbf{r}) = N - D(\mathbf{r})$ additional DoF will be sensed by internal user at coordinates $\mathbf{r}$ and not occupied by external-network transmissions. These $K(\mathbf{r})$ DoF are contained in the so-called *noise subspace*, namely $\mathcal{N}(\mathbf{r})$. This subspace is orthogonal to $\mathcal{S}(\mathbf{r})$. Given this geometrical interpretation, if opportunistic transmissions belong to $\mathcal{N}(\mathbf{r})$ all inter-system interferences will be (ideally) avoided. In other words, imagine that a basis of $\mathcal{S}(\mathbf{r})$, namely $\mathbf{\Psi}_{\mathcal{S}}(\mathbf{r})$, can be obtained via some sensing mechanism, which is beyond the scope of this work. Furthermore, let $\boldsymbol{\varphi}(\mathbf{r})$ be the opportunistic waveform to be designed at some node located at coordinates $\mathbf{r}$. The design problem addressed in this work can be expressed as

$$\mathbf{\Psi}_{\mathcal{S}}(\mathbf{r})^{H}\boldsymbol{\varphi}(\mathbf{r}) = \mathbf{0}. \tag{4}$$

That is, if *complete side information* of signal subspace (i.e. a basis) is available at an arbitrary internal node, it can adapt its transmissions to be orthogonal to $\mathcal{S}(\mathbf{r})$. Therefore, these transmissions will see external-network interferences as noise, and vice-versa. Nevertheless, a complete knowledge of $\mathbf{\Psi}_{\mathcal{S}}(\mathbf{r})$ is not always possible, due to the locality of external-network observations, sensing errors and monitoring conditions. In general, we refer to these effects as *sensing uncertainties*.

A. Local Sensing Uncertainties: A Mathematical Model

Recalling the design problem stated in (4), the complete knowledge of a signal-subspace basis is needed to appropriately design the opportunistic waveform. Yet in practice, subspaces sensed at each user may slightly differ. On the one hand, each internal node may suffer from sensing errors. These errors depend on the particular sensing mechanism used by each node and are scenario-independent. On the other hand, we have to account for multipath and shadow fading, and the outage of interference channels. Regarding to Fig. 2, signal and noise subspaces can be written as

$$\mathcal{S}(\mathbf{r}) = \tilde{\mathcal{S}}(\mathbf{r}) \cup \mathcal{S}_{\mathcal{E}}(\mathbf{r}), \tag{5}$$

$$\mathcal{N}(\mathbf{r}) = \tilde{\mathcal{N}}(\mathbf{r}) \cup \mathcal{N}_{\mathcal{E}}(\mathbf{r}), \tag{6}$$

which are respectively spanned by orthonormal bases

$$\mathbf{\Psi}_{\mathcal{S}}(\mathbf{r}) = \left[\begin{array}{c:c} \tilde{\mathbf{\Psi}}_{\mathcal{S}}(\mathbf{r}) & \mathbf{\Xi}(\mathbf{r}) \end{array}\right], \tag{7}$$

$$\mathbf{\Psi}_{\mathcal{N}}(\mathbf{r}) = \left[\begin{array}{c:c} \tilde{\mathbf{\Psi}}_{\mathcal{N}}(\mathbf{r}) & \mathbf{\Upsilon}(\mathbf{r}) \end{array}\right]. \tag{8}$$

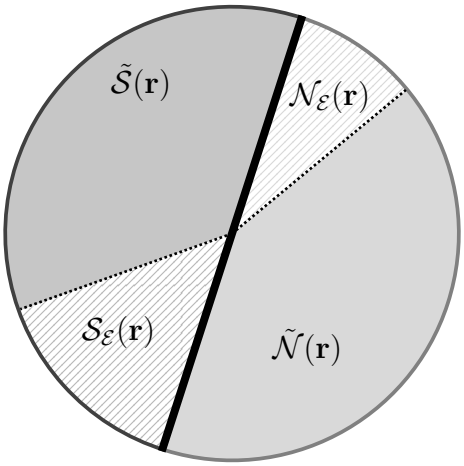

Fig. 2: Graphical representation of signal and noise subspaces at arbitrary geographical coordinates $\mathbf{r}$ and their partitions, respectively.

When local sensing uncertainties are taken into consideration, internal-network nodes are not able to obtain the bases (7) and (8). Contrarily, the bases sensed by opportunistic nodes via an arbitrary sensing mechanism are given by

$$\hat{\mathbf{\Psi}}_{\mathcal{S}}(\mathbf{r}) = \left[\begin{array}{c:c} \tilde{\mathbf{\Psi}}_{\mathcal{S}}(\mathbf{r}) & \mathbf{\Upsilon}(\mathbf{r}) \end{array} \right], \tag{9}$$

$$\hat{\mathbf{\Psi}}_{\mathcal{N}}(\mathbf{r}) = \left[\begin{array}{c:c} \tilde{\mathbf{\Psi}}_{\mathcal{N}}(\mathbf{r}) & \mathbf{\Xi}(\mathbf{r}) \end{array} \right]. \tag{10}$$

Notice that $\tilde{\mathcal{S}}(\mathbf{r}) = \text{span}[\tilde{\mathbf{\Psi}}_{\mathcal{S}}(\mathbf{r})]$ and $\tilde{\mathcal{N}}(\mathbf{r}) = \text{span}[\tilde{\mathbf{\Psi}}_{\mathcal{N}}(\mathbf{r})]$ contain the DoF correctly sensed as occupied and available, respectively, whereas $\mathcal{S}_{\mathcal{E}}(\mathbf{r}) = \text{span}[\mathbf{\Xi}(\mathbf{r})]$ and $\mathcal{N}_{\mathcal{E}}(\mathbf{r}) = \text{span}[\mathbf{\Upsilon}(\mathbf{r})]$ encompass those occupied and available DoF erroneously sensed as available and occupied, respectively. Thus, we can define the dimensions of (9) and (10) as

$$\hat{D}(\mathbf{r}) = D(\mathbf{r}) - \epsilon(\mathbf{r}) - \delta(\mathbf{r}) + \left(K(\mathbf{r}) - \tilde{K}(\mathbf{r}) \right), \tag{11}$$

$$\hat{K}(\mathbf{r}) = \tilde{K}(\mathbf{r}) + \epsilon(\mathbf{r}) + \delta(\mathbf{r}), \tag{12}$$

where $\tilde{K}(\mathbf{r})$ is the number of available DoF sensed as available, $\delta(\mathbf{r})$ is the number of occupied DoF sensed as available due to poor monitoring conditions, and $\epsilon(\mathbf{r})$ is the number of occupied DoF sensed as available accounting for the sensing errors. Notice that $\tilde{K}(\mathbf{r}) \leq K(\mathbf{r})$ due to the false-alarm probability P_{FA} of the considered sensing mechanism.

It is worth noting that, according to (11) and (12), the dimensions of subspaces depicted in Fig. 2 are

$$\tilde{K}(\mathbf{r}) = \dim[\tilde{\mathcal{N}}(\mathbf{r})] \tag{13}$$

$$K(\mathbf{r}) - \tilde{K}(\mathbf{r}) = \dim[\mathcal{N}_{\mathcal{E}}(\mathbf{r})] \tag{14}$$

$$\xi(\mathbf{r}) = \epsilon(\mathbf{r}) + \delta(\mathbf{r}) = \dim[\mathcal{S}_{\mathcal{E}}(\mathbf{r})] \tag{15}$$

$$D(\mathbf{r}) - \xi(\mathbf{r}) = \dim[\tilde{\mathcal{S}}(\mathbf{r})] \tag{16}$$

As a consequence of these sensing uncertainties, we will observe different effects at internal transmitter and receiver, which will be discussed in Sec. VI. In summary, opportunistic communication always suffer from energy loss and/or noise enhancement. Inter-system interferences to (from) external network are only present when transmitter (receiver) detects as available a DoF which is occupied by an external-network user and sensing conditions are favorable. Since internal-network node at coordinates $\mathbf{r}$ is not able to avoid the effects of these sensing uncertainties, the best that can be done is to prevent internal-network users from interfere the occupied DoF correctly sensed, i.e. the ones belonging to $\tilde{\mathbf{\Psi}}_{\mathcal{S}}(\mathbf{r})$, and minimize the impact on those DoF encompassed in $\mathbf{\Xi}(\mathbf{r})$.

III. Main Result

In this Section, we present the main contribution of this work and its properties as well. Taking into account the previous discussion on local sensing uncertainties, yet in practice, it is not possible to use an *actual* signal-subspace basis. In the sequel, the shaping filter under worst-case local sensing uncertainties conditions is given in Theorem 1:

Theorem 1. *Let* $\hat{\mathbf{P}}_{\mathcal{N}}(\mathbf{r}) \triangleq \hat{\mathbf{\Psi}}_{\mathcal{N}}(\mathbf{r})\hat{\mathbf{\Psi}}_{\mathcal{N}}^{H}(\mathbf{r})$ *be an orthogonal projector onto the sensed noise subspace at arbitrary coordinates* $\mathbf{r}$ *such that the elements of its main diagonal are sorted in decreasing order. Then, the shaping filter is given by*

$$\hat{\boldsymbol{\varphi}}_1 = \left(\mathbf{e}_1^H \hat{\mathbf{P}}_{\mathcal{N}}(\mathbf{r})\mathbf{e}_1\right)^{-1/2} \hat{\mathbf{P}}_{\mathcal{N}}(\mathbf{r})\mathbf{e}_1, \tag{17}$$

where

$$\mathbf{e}_n \triangleq \left[\mathbf{0}_{n-1}^T \; 1 \; \mathbf{0}_{N-n}^T\right]^T \in \mathbb{C}^N. \tag{18}$$

From the N *columns of* $\hat{\mathbf{P}}_{\mathcal{N}}(\mathbf{r})$*, the one containing the maximum value of its main diagonal is the optimum solution in terms of minimum inter-system interference per DoF. The given solution is independent of the chosen basis* $\hat{\mathbf{\Psi}}_{\mathcal{N}}(\mathbf{r})$.

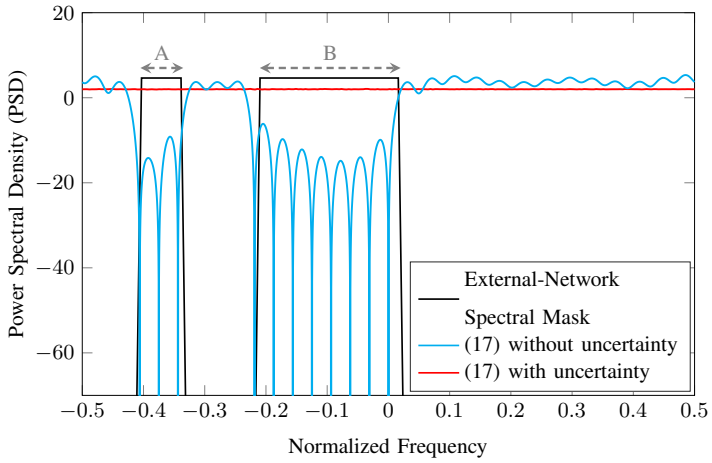

Fig. 3: PSD of proposed signaling scheme (17) in a proof-of-concept (useless) case with a very low subspace dimension ($N = 32$ DoF).

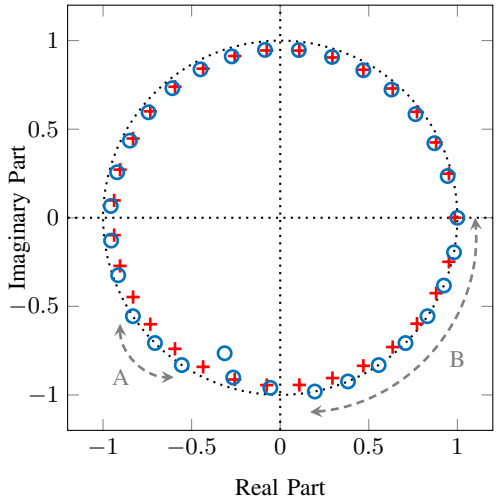

Fig. 4: Zeros distribution of (17) without uncertainty (blue circles) and with maximum uncertainty (red crosses).

It is worth noticing that, if the solution is unique, the *optimum* shaping filter is the first column of $\hat{\mathbf{P}}_{\mathcal{N}}(\mathbf{r})$. Nevertheless, if multiple solutions exist, detection ambiguities arise. Even though it can be seen as a disadvantage in view of signal detectability, it is an inherent advantage in terms of *waveform diversity*, which is of paramount importance in multiuser scenarios. The problem of multiple solutions will be exploited in Sec. VII. The opened question, addressed in Proposition 1, is when the solution's uniqueness can be guaranteed.

Proposition 1 (Solution's Uniqueness)**.** *Let* $p_k \triangleq [\hat{\mathbf{P}}_{\mathcal{N}}(\mathbf{r})]_{kk}$ *be the* k*-th diagonal entry of* $\hat{\mathbf{P}}_{\mathcal{N}}(\mathbf{r})$*. The solution presented in Theorem 1 will be unique if and only if*

$$p_1 > p_k, \text{ for } k = 2, \ldots, N. \tag{19}$$

Otherwise, when the main diagonal of $\hat{\mathbf{P}}_{\mathcal{N}}(\mathbf{r})$ *presents more than one maximum, i.e.*

$$p_1 = p_k > p_{N-k} \geq p_N \textit{ for } k \in [2, N], \tag{20}$$

the solution is not unique yielding selection ambiguities.

Recalling Theorem 1, the proposed shaping filter relies on the orthogonal projector onto the sensed noise subspaces. Thus, as further analyzed in Sec. V, (17) exhibits:

(i) Invariance to Noise-Subspace Rotations
(ii) Robustness in front of frequency and/or phase offsets
(iii) Uniform Distribution of Zero's Shaping Filter

These properties are of paramount importance in this work, since they guarantee that the unintended inter-system interference per DoF is minimum and the waveform's detectability by neighboring nodes.

As a final remark on the shaping scheme proposed in this work, it is important to notice that both internal-network transmitting and receiving nodes will design their filters using only local external-network observations, i.e. without end-to-end coordination. Hence, the following observation arises:

Proposition 2 (Solution's Symmetry)**.** *Under the lack of end-to-end coordination, the strategy employed by receiver to be aware of the presence of any potential transmitting node is completely symmetric to that employed by transmitter to minimize the undesired impact on external network.*

A. Proof-of-Concept

Before going deeper into the mathematical analysis, we provide a proof-of-concept example to illustrate the behavior of the proposed shaping scheme. To that end, we have considered that basis $\hat{\mathbf{\Psi}}_{\mathcal{N}}(\mathbf{r})$ is a subset of the Fourier matrix of size N. This subset is assumed to be identified by an arbitrary sensing mechanism. In this case, the concept of DoF refers to carriers. For the sake of illustration, we have considered a *useless* case with $N = 32$ DoF (carriers). A fraction of $3/8$ of N is detected as occupied. For simplicity, we consider two extreme cases, i.e. when there is no sensing uncertainties and when sensing uncertainties are maximum. The *spectral* behavior of (17) is depicted in Figs. 3 and 4. Notice that the solution presented in Theorem 1 forces zeros when a carrier is sensed as occupied and tries to uniformly used those carriers sensed as available. In case of maximum uncertainty, all ($N = 32$) carriers are uniformly exploited. Thus,

(17) tries to perform a uniform power allocation among DoF detected as available. In other words, the filter's zeros associated with those DoF are uniformly distributed in a constant radius circle (see Fig. 4).

IV. Decentralized Signaling Design Scheme

Thus far, we have presented the main result of this work, a scenario-aware pulse shaping design scheme. This Section is devoted to formally deriving the result in Theorem 1. To that end, we address the design at arbitrary geographical coordinates $\mathbf{r}$. Nevertheless, for simplicity of notation, we drop the dependence on $\mathbf{r}$ whenever it is possible.

Bearing in mind the discussion on local sensing uncertainties in Sec. II-A, full knowledge of an *actual* signal-subspace basis is not possible in general. Thus, since some occupied DoF will be sensed as available, we will consider the worst-case scenario. That is, we look for a shaping filter $\boldsymbol{\varphi}$ orthogonal to the *sensed* signal subspace $\hat{\mathcal{S}} = \tilde{\mathcal{S}} \cup \mathcal{N}_{\mathcal{E}}$ (spanned by $\hat{\boldsymbol{\Psi}}_{\mathcal{S}}$ in (9)) and with minimum impact on those DoF encompassed in $\mathcal{S}_{\mathcal{E}}$ (spanned by $\boldsymbol{\Xi}$). To that end, let us define the *extended* signal-subspace basis as

$$\breve{\boldsymbol{\Psi}}_{\mathcal{S}} = \left[\begin{array}{c:c} \hat{\boldsymbol{\Psi}}_{\mathcal{S}} & \boldsymbol{\Xi} \end{array} \right]. \tag{21}$$

Recalling the waveform design problem stated in (4) and the decomposition of the extended signal-subspace basis in (21), the shaping filter design becomes

$$\left[\begin{array}{c:c} \hat{\boldsymbol{\Psi}}_{\mathcal{S}} & \boldsymbol{\Xi} \end{array} \right]^H \boldsymbol{\varphi} = \mathbf{0} + \mathbf{e}_{\mathcal{S}}, \tag{22}$$

where $\mathbf{e}_{\mathcal{S}}$ is an error vector belonging to the span of $\boldsymbol{\Xi}$, i.e. non-orthogonal to those occupied DoF sensed as available. By defining the following matrices

$$\hat{\boldsymbol{\Omega}}_{\mathcal{S}}^H = \left[\begin{array}{c:c} \hat{\boldsymbol{\Psi}}_{\mathcal{S}} & \mathbf{0}_{N \times \xi} \end{array} \right], \tag{23}$$

$$\mathbf{E}_{\mathcal{S}}^H = \left[\begin{array}{c:c} \mathbf{0}_{N \times \hat{D}} & \boldsymbol{\Xi} \end{array} \right], \tag{24}$$

the design problem in (22) can be formulated as

$$\left(\hat{\boldsymbol{\Omega}}_{\mathcal{S}} + \mathbf{E}_{\mathcal{S}} \right) \boldsymbol{\varphi} = \mathbf{0} + \mathbf{e}_{\mathcal{S}}, \tag{25}$$

or, equivalently,

$$\left(\left[\begin{array}{c:c} \mathbf{0} & \hat{\boldsymbol{\Omega}}_{\mathcal{S}} \end{array} \right] + \left[\begin{array}{c:c} \mathbf{e}_{\mathcal{S}} & \mathbf{E}_{\mathcal{S}} \end{array} \right] \right) \left[\begin{array}{c} -1 \\ \boldsymbol{\varphi} \end{array} \right] = \mathbf{0}. \tag{26}$$

It is worth noticing that, thanks to the additive model in (25), the pulse shaping filter design problem admits a total least-squares (TLS) formulation [43], where $\mathbf{E}_{\mathcal{S}}$ and $\mathbf{e}_{\mathcal{S}}$ represent the errors in data matrix and observations vector, respectively. According to [43], (26) admits the following formulation:

$$\min_{\{\mathbf{E}_{\mathcal{S}},\mathbf{e}_{\mathcal{S}}\}} \left\| \left[\begin{array}{c:c} \mathbf{e}_{\mathcal{S}} & \mathbf{E}_{\mathcal{S}} \end{array} \right] \right\|_{\mathrm{F}}^2 \tag{27a}$$

$$\text{subject to } \left(\hat{\boldsymbol{\Omega}}_{\mathcal{S}} + \mathbf{E}_{\mathcal{S}}\right) \boldsymbol{\varphi} = \mathbf{0} + \mathbf{e}_{\mathcal{S}}. \tag{27b}$$

Following the rationale in [43–46], we have to find a solution orthogonal to $\mathbf{T}^H\mathbf{T}$, being $\mathbf{T}$ the extended data matrix:

$$\mathbf{T} = \left[\begin{array}{c:c} \mathbf{0} & \hat{\boldsymbol{\Omega}}_{\mathcal{S}} \end{array} \right] \in \mathbb{C}^{\hat{D}\times(N+1)}. \tag{28}$$

It is worth noting that $\mathbf{T}$ is a rank-deficient matrix with $\mathrm{rank}(\mathbf{T}) = \mathrm{rank}(\hat{\boldsymbol{\Omega}}_{\mathcal{S}}) = D - \xi$. Thus, taking into account the singular value decomposition (SVD) of (28), viz.

$$\mathbf{T} = \left[\begin{array}{c:c} \mathbf{U}_1 & \mathbf{U}_2 \end{array} \right] \left[\begin{array}{cc:c} \boldsymbol{\Sigma}_1 & & \\ & \boldsymbol{\Sigma}_2 & \mathbf{0} \end{array} \right] \left[\begin{array}{c} \mathbf{V}_1^H \\ \hdashline \\ \mathbf{V}_2^H \end{array} \right], \tag{29}$$

the null-space of $\mathbf{T}^H\mathbf{T}$ is spanned by $\mathbf{V}_2$. Classically, the following partition of $\mathbf{V}_2$ is considered

$$\mathbf{V}_2^T = \left[\begin{array}{c:c} \mathbf{c} & \tilde{\mathbf{V}}_2^T \end{array} \right]. \tag{30}$$

Therefore, taking into account the derivation in [45], the TLS waveform leads to

$$\boldsymbol{\varphi}_{\text{TLS}} = \left(\mathbf{c}^H\mathbf{c}\right)^{-1} \tilde{\mathbf{V}}_2\mathbf{c}^*. \tag{31}$$

When the null-space of $\mathbf{T}^H\mathbf{T}$ has dimension greater than one, notice that the solution is not unique, i.e. (30) is not unique. In that case the solution which has minimum norm should be selected. Yet, if multiple minimum-norm solutions exist, internal-network users can arbitrarily select any of the them, yielding detection uncertainties at receiver side.

By carefully analyzing (31), it is straightforward to conclude that it corresponds to the first column of orthogonal projector onto the null-space of $\mathbf{T}^H\mathbf{T}$, whenever the solution is unique. Hence, by noticing that

$$\mathbf{T}^H\mathbf{T} = \left[\begin{array}{cc} 0 & \mathbf{0}_{1\times N} \\ \mathbf{0}_{N\times 1} & \hat{\boldsymbol{\Psi}}_{\mathcal{S}}\hat{\boldsymbol{\Psi}}_{\mathcal{S}}^H \end{array} \right], \tag{32}$$

proposed solution in (31) is nothing but the first column of $\mathbf{I}_N - \hat{\boldsymbol{\Psi}}_{\mathcal{S}}\hat{\boldsymbol{\Psi}}_{\mathcal{S}}^H = \hat{\boldsymbol{\Psi}}_{\mathcal{N}}\hat{\boldsymbol{\Psi}}_{\mathcal{N}}^H \triangleq \hat{\mathbf{P}}_{\mathcal{N}}$, as presented in Theorem 1.

A. *Equivalence of* (31) *and Minimum-Norm*

Since TLS designs a solution robust to both errors in data matrix and observations vector, (31) is the most robust solution in front of sensing uncertainties. Yet, we also may address the design problem as a min-max optimization:

$$\min_{\boldsymbol{\varphi}} \ \max_{\boldsymbol{\Xi}} \ \left\| \left[\ \hat{\boldsymbol{\Psi}}_{\mathcal{S}} \ \vdots \ \boldsymbol{\Xi} \ \right]^{H} \boldsymbol{\varphi} \right\|_2^2 . \tag{33}$$

Nevertheless, the cost function in (33) will be constrained to avoid the trivial solution and limit the maximum "uncertainty". Regarding to the former, we will consider the so-called linear predictor condition [47], [48] as a non-trivial design constraint. Concerning the latter, because the uncertainty is defined as the number of DoF encompassed in $\boldsymbol{\Xi}$, we upper-bound the rank of matrix $\boldsymbol{\Xi}$. Thus, the complete waveform design problem under worst-case sensing uncertainties is written as

$$\min_{\boldsymbol{\varphi}} \ \max_{\boldsymbol{\Xi}} \qquad \left\| \left[\ \tilde{\boldsymbol{\Psi}}_{\mathcal{S}} \ \vdots \ \boldsymbol{\Xi} \ \right]^{H} \boldsymbol{\varphi} \right\|_2^2 \tag{34a}$$

$$\text{subject to} \ \ \operatorname{rank}(\boldsymbol{\Xi}) \leq \epsilon \ \text{ and } \ \mathbf{e}_n^H \boldsymbol{\varphi} = \alpha \tag{34b}$$

where $\epsilon \in \mathbb{Z}_+ \backslash \{0\}$, $\alpha \in \mathbb{R}_+ \backslash \{0\}$ and $\mathbf{e}_n$ is defined as in (18) (see Theorem 1). The maximization problem in (34a)–(34b) yields a rank-one worst-case matrix $\boldsymbol{\Xi}$ such that all energy transmitted through the opportunistic channel will corrupt one occupied DoF sensed as available. Under this pessimistic conditions, the minimization in (34a)–(34b) yields

$$\hat{\boldsymbol{\varphi}}_1 = \left(\mathbf{e}_1^H \hat{\boldsymbol{\Psi}}_{\mathcal{N}} \hat{\boldsymbol{\Psi}}_{\mathcal{N}}^H \mathbf{e}_1 \right)^{-1/2} \hat{\boldsymbol{\Psi}}_{\mathcal{N}} \hat{\boldsymbol{\Psi}}_{\mathcal{N}}^H \mathbf{e}_1 . \tag{35}$$

As discussed in Sec. III, whether the main diagonal of the orthogonal projector $\hat{\mathbf{P}}_{\mathcal{N}} \triangleq \hat{\boldsymbol{\Psi}}_{\mathcal{N}} \hat{\boldsymbol{\Psi}}_{\mathcal{N}}^H$ is sorted in decreasing order, the solution in (35) is given by $n = 1$.

It is worth noting that design scheme presented in this subsection obeys a minimum-norm optimization [47], [48]. Therefore, even all columns of $\hat{\mathbf{P}}_{\mathcal{N}}$ are orthogonal to the *sensed* signal subspace, the one which contains the maximum value of the main diagonal of $\hat{\mathbf{P}}_{\mathcal{N}}$ is the minimum-norm solution of the design problem. Hence, and recalling the discussion in (32), it is equivalent to seek the *optimum* waveform in (31) or in (35). Actually, this result is not surprising at all. As stated in [45], minimum-norm and TLS are equivalent, and as also reported, the solution can be found either with the signal-subspace or the noise-subspace projector, thanks to the duality between these subspaces.

B. Solution's Robustness

It is worth noticing that, according to (10), the sensed noise-subspace basis can be expressed as

$$\hat{\mathbf{\Psi}}_{\mathcal{N}} = \left[\begin{array}{c:c} \tilde{\mathbf{\Psi}}_{\mathcal{N}} & \mathbf{\Xi} \end{array} \right]. \tag{36}$$

Hence, by definition, $\tilde{\mathcal{N}} \subseteq \mathcal{N}$, where the equality only holds whenever $\tilde{K} = K$. Therefore, the waveform designed in (31) does not belong to $\tilde{\mathcal{N}}$, and in turn, to $\mathcal{N}$. However, since it belongs to $\hat{\mathcal{N}}$, the orthogonality to the actual signal subspace $\mathcal{S}$ cannot be guaranteed. Recall that this waveform has been designed to be orthogonal to $\hat{\mathcal{S}}$. Nevertheless, as proved herein, the proposed design scheme is the best that can be done under sensing uncertainties. Taking into consideration the structure of sensed noise-subspace basis in (36), the designed waveform (31) can be written as

$$\hat{\boldsymbol{\varphi}}_n = \boldsymbol{\varphi}_n^{\mathcal{N}} + \boldsymbol{\varphi}_n^{\perp}, \tag{37}$$

with $\boldsymbol{\varphi}_n^{\mathcal{N}} \in \tilde{\mathcal{N}}$ being the desired solution and $\boldsymbol{\varphi}_n^{\perp} \in \mathcal{S}_{\mathcal{E}}$ standing for an error induced by sensing uncertainties. In this view, matrix $\mathbf{\Xi}$ in (36) can be seen as an error in the noise-subspace basis. By following the same rationale than in (22)–(26), we have that

$$\left(\left[\begin{array}{c:c} \boldsymbol{\varphi}_n^{\mathcal{N}} & \tilde{\mathbf{\Omega}}_{\mathcal{N}} \end{array} \right] + \left[\begin{array}{c:c} \boldsymbol{\varphi}_n^{\perp} & \mathbf{E}_{\mathcal{N}} \end{array} \right] \right) \left[\begin{array}{c} -1 \\ \boldsymbol{\lambda} \end{array} \right] = \mathbf{0}. \tag{38}$$

Hence, the linear combination coefficients $\boldsymbol{\lambda}$ can be found to jointly minimize the impact of the errors $\boldsymbol{\varphi}_n^{\perp}$ and $\mathbf{E}_{\mathcal{N}}$ as

$$\min_{\{\mathbf{E}_{\mathcal{N}}, \boldsymbol{\varphi}_n^{\perp}, \boldsymbol{\lambda}\}} \left\| \left[\begin{array}{c:c} \boldsymbol{\varphi}_n^{\perp} & \mathbf{E}_{\mathcal{N}} \end{array} \right] \right\|_{\mathrm{F}}^2 \tag{39a}$$

$$\text{subject to } \left(\tilde{\mathbf{\Omega}}_{\mathcal{N}} + \mathbf{E}_{\mathcal{N}} \right) \boldsymbol{\lambda} = \boldsymbol{\varphi}_n^{\mathcal{N}} + \boldsymbol{\varphi}_n^{\perp}. \tag{39b}$$

It is worth noting that the cost function in (39a) reduces to

$$\left\| \left[\begin{array}{c:c} \boldsymbol{\varphi}_n^{\perp} & \mathbf{E}_{\mathcal{N}} \end{array} \right] \right\|_{\mathrm{F}}^2 = \left\| \boldsymbol{\varphi}_n^{\perp} \right\|_{\mathrm{F}}^2 + (\epsilon + \delta), \tag{40}$$

meaning that, for fixed DoF excesses ϵ and δ [cf. (12)], the proposed design scheme minimizes the impact on those DoF which have been incorrectly sensed as available. Thus, as aforementioned in Theorem 1, we observe the following:

Proposition 3 (Minimum Inter-System Interference per DoF)**.** *Since the power transmitted is uniformly distributed among the $\hat{K} = \tilde{K} + \xi$ sensed available DoF and, according to* (40)*, the power injected to* $\mathrm{span}[\mathbf{\Xi}]$ *is minimized, the inter-system interference per DoF is minimum.*

Proof. See Appendix A. ■

V. Analysis of Solution Properties

In the previous Section, we have formally derived the optimal signaling pattern in the sense of minimum inter-system interference per DoF. In this Section, we are going to analyze the properties of the derived solution in (17), previously stated in Sec. III. Some of these properties were partially analyzed by the authors in [49], [50].

A. Invariance to Noise-Subspace Rotations

Recall that the derived solution (31) relies on the orthogonal projector onto the noise subspace. In comparison with other noise-subspace solutions found in the literature, all of them are orthogonal to the sensed signal subspace. A well-identified problem in orthogonal opportunistic transmission is the ambiguity of adopted noise-subspace bases at each internal-network node. While this ambiguity is inherent in those solutions relying on the noise-subspace bases due to the lack of rotational invariance, it is overcome in our solution.

Let $\mathbf{U} \in \mathbb{C}^{\hat{K}\times N}$ be a unitary matrix. We define a rotated noise-subspace basis as $\hat{\mathbf{\Psi}}_{\mathcal{N}}^{(r)} \triangleq \hat{\mathbf{\Psi}}_{\mathcal{N}}\mathbf{U}$. Notice that this rotation occurs within the noise subspace. Hence, the orthogonal projector results unaffected by this rotation:

$$\hat{\mathbf{P}}_{\mathcal{N}}^{(r)} = \hat{\mathbf{\Psi}}_{\mathcal{N}}^{(r)}\left(\hat{\mathbf{\Psi}}_{\mathcal{N}}^{(r)}\right)^{H} = \hat{\mathbf{\Psi}}_{\mathcal{N}}\mathbf{U}\mathbf{U}^{H}\hat{\mathbf{\Psi}}_{\mathcal{N}}^{H} = \hat{\mathbf{P}}_{\mathcal{N}}. \tag{41}$$

This property is of paramount importance since guarantees coherent waveform detection, exhibiting a better detection performance than those schemes relying on the basis itself. Among other cases, this property is very interesting to overcome ambiguities when covariance-based sensing schemes are employed and noise-eigenvalues' multiplicity is greater than 1.

B. Invariance to Phase and/or Frequency errors

Notice that an inefficient backbone infrastructure is not needed in decentralized communication systems. Nevertheless, there is another important advantage. Since opportunistic nodes only account for local observations of the wireless environment, each opportunistic node chooses its own reference, such that they locally calibrate theirselves. Mathematically, let us consider that matrix $\mathbf{\Gamma}$ contains the reference errors in its main diagonal, i.e.

$$\mathbf{\Gamma} = \mathrm{diag}(\exp\{j2\pi\upsilon_0 + \phi_0\}, \ldots, \exp\{j2\pi N\upsilon_0 + \phi_0\}). \tag{42}$$

Since orthogonal projector is not affected by (42), the proposed pulse shaping filters are robust in front of offsets, as any other decentralized waveform design scheme.

C. Distribution of Waveform's Zeros

Recall that proposed pulse shaping filters are the result of the double optimization problem in (34a), subject to constraints (34b). Once the worst-case matrix $\boldsymbol{\Xi}$ is obtained, the design problem reduces to the following constrained minimization. Hence, for $\alpha = 1$, we have that

$$\hat{\boldsymbol{\varphi}}_n = \arg\min_{\boldsymbol{\varphi}} \|\boldsymbol{\varphi}\|_2^2 \;\; \text{subject to} \;\; \mathbf{e}_n^H \boldsymbol{\varphi} = 1, \; \boldsymbol{\varphi} \in \hat{\mathcal{N}}(\mathbf{r}). \tag{43}$$

Equivalently, by means of the Parseval's Theorem, the cost function in (43) can be addressed in the transformed domain. For ease of notation, let $\Phi(z)$ be the $\mathcal{Z}$-transform of $\boldsymbol{\varphi}$. Hence, by denoting C_1 and C_2 two simple contour encircling counterclockwise the origin, (43) yields

$$\frac{\|\boldsymbol{\varphi}\|^2}{|\mathbf{e}_n^H \boldsymbol{\varphi}|^2} = \frac{\dfrac{1}{j2\pi} \oint_{C_1} |\Phi(z)|^2 \dfrac{\mathrm{d}z}{z}}{\left| \dfrac{1}{j2\pi} \oint_{C_2} \Phi(z) \left(\dfrac{1}{z^*} \right)^{-n} \dfrac{\mathrm{d}z}{z} \right|^2} \geq \frac{1}{|z^n|^2}. \tag{44}$$

Therefore, the zeros of $\Phi(z)$ are almost uniformly distributed inside the unit circle. In other words, transmitted power will be asymptotically uniformly distributed. This result is of paramount importance because if a DoF is incorrectly used, the amount of injected power will not be so high, but exactly the same as in the remaining ones. As a last comment, this result is apparently not surprising. Recall that the design scheme presented in this work can be seen as a minimum-norm optimization problem. Kumaresan intuitively proved in [51] that the so-called *extraneous* zeros of a minimum-norm filter will be almost uniformly distributed in the unit circle. Hence, the derivation in (44) can be seen as a formal argument of the result presented in [51].

VI. End-to-End Approach

Heretofore, we have discussed the design of context-aware shaping filters at arbitrary geographical coordinates $\mathbf{r}$ and their properties. Nonetheless, since the objective is to setup a communication link, we have to analyze whether the signaling locally designed at transmitter can be detected at the receiver side in an uncoordinated manner.

Recall that each internal-network node constructs a noise-subspace basis accounting solely for local observations from the wireless environment. Thus, noise subspaces sensed at each internal

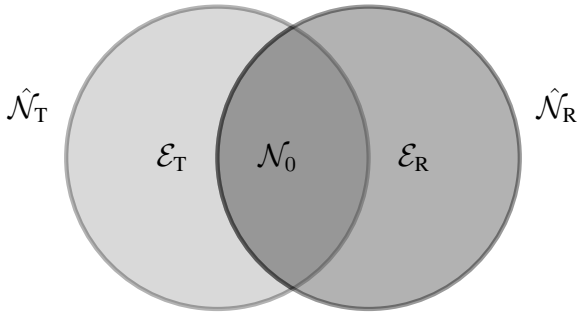

Fig. 5: Graphical representation of the relation between noise subspaces at internal transmitting and receiving nodes $\hat{\mathcal{N}}_{\mathrm{T}}$ and $\hat{\mathcal{N}}_{\mathrm{R}}$, respectively.

node may differ. Although the dimension of these subspaces may be equal (which is not the general case), only a portion of these subspaces will match. This portion is denoted as *effective noise subspace*.

Definition 1 (Effective Noise Subspace)**.** *Let $\hat{\mathcal{N}}_T \triangleq \hat{\mathcal{N}}(\mathbf{r} = \mathbf{r}_T)$ and $\hat{\mathcal{N}}_R \triangleq \hat{\mathcal{N}}(\mathbf{r} = \mathbf{r}_R)$ be the noise subspaces sensed at internal transmitting (T) and receiving (R) nodes, being $\hat{K}_T \triangleq \hat{K}(\mathbf{r} = \mathbf{r}_T)$ and $\hat{K}_R \triangleq \hat{K}(\mathbf{r} = \mathbf{r}_R)$ their dimensions, respectively. The effective noise subspace $\mathcal{N}_0$ is defined as*

$$\mathcal{N}_0 \triangleq \hat{\mathcal{N}}_T \cap \hat{\mathcal{N}}_R, \tag{45}$$

whose dimension is, in general, $K_0 \leq \min\{\tilde{K}_T, \tilde{K}_R\}$. Additionally, given the independence of sensing channels and sensing errors at different nodes, $\mathcal{N}_0 \subseteq \mathcal{N}(\mathbf{r})$ with high probability.

Therefore, taking into account Definition 1 and Fig. 5, the sensed noise subspace at any arbitrary internal-network node can be decomposed as

$$\hat{\mathcal{N}}(\mathbf{r}) = \mathcal{N}_0 \cup \mathcal{E}(\mathbf{r}), \tag{46}$$

where $\mathcal{N}_0$ contains the DoF that are simultaneously used by transmitting and receiving nodes, whereas $\mathcal{E}(\mathbf{r})$ encompasses those DoF solely used by transmitting or receiving node. In the sequel, $\kappa(\mathbf{r})$ denotes the dimension of $\mathcal{E}(\mathbf{r})$. As a final remark on (46), it follows that

$$\mathcal{N}_0 \cap \mathcal{E}(\mathbf{r}) = \emptyset \tag{47}$$

$$\mathcal{E}(\mathbf{r}') \cap \mathcal{E}(\mathbf{r}) = \emptyset, \ \forall \mathbf{r} \neq \mathbf{r}'. \tag{48}$$

It is worth noting that the decomposition in (46) is only well-defined in the pairwise sense. Taking these new details into consideration, we see that sensing uncertainties may incur in a performance

Table I: Effects of sensing uncertainties at each internal node.

	Internal Transmitter	**Internal Receiver**
$\tilde{K}(\mathbf{r}) - K_0$	Energy Loss	Noise Enhancement
$\delta(\mathbf{r})$		
$\epsilon(\mathbf{r})$	Energy Loss and Interference to External Network	Noise Enhancement and Interference from External Network

loss in both internal and external systems, depending on the origin of these uncertainties (see Sec. III). The effects on the overall performance of false-alarm rate, monitoring conditions and miss detection at internal transmitting and receiving nodes are summarized in Table I.

Bearing in mind the previous discussion, we may decompose the orthogonal projector onto $\hat{\mathcal{N}}(\mathbf{r})$ as

$$\hat{\mathbf{P}}_{\mathcal{N}}(\mathbf{r}) = \hat{\mathbf{P}}_{\mathcal{N}_0} + \hat{\mathbf{P}}_{\mathcal{E}(\mathbf{r})}. \tag{49}$$

Therefore, the n-th waveform designed at node $\mathbf{r}$ is given by

$$\hat{\boldsymbol{\varphi}}_n(\mathbf{r}) = \left(\mathbf{e}_n^H \left[\hat{\mathbf{P}}_{\mathcal{N}_0} + \hat{\mathbf{P}}_{\mathcal{E}(\mathbf{r})}\right] \mathbf{e}_n\right)^{-\frac{1}{2}} \left[\hat{\mathbf{P}}_{\mathcal{N}_0} + \hat{\mathbf{P}}_{\mathcal{E}(\mathbf{r})}\right] \mathbf{e}_n. \tag{50}$$

In the sequel, we denote $\hat{\boldsymbol{\varphi}}_{\mathrm{T}} \triangleq \hat{\boldsymbol{\varphi}}_n(\mathbf{r} = \mathbf{r}_{\mathrm{T}})$ and $\hat{\boldsymbol{\varphi}}_{\mathrm{R}} \triangleq \hat{\boldsymbol{\varphi}}_n(\mathbf{r} = \mathbf{r}_{\mathrm{R}})$ the waveforms designed at internal transmitting and receiving nodes. For the sake of simplicity, let us assume that the solution in unique at both internal nodes. When $\hat{\boldsymbol{\varphi}}_{\mathrm{R}}$ is used as a matched-filter detector, we see that

$$\hat{\boldsymbol{\varphi}}_{\mathrm{R}}^H \hat{\boldsymbol{\varphi}}_{\mathrm{T}} = \frac{\mathbf{e}_{\mathrm{R}}^H \hat{\mathbf{P}}_{\mathcal{N}_0} \hat{\mathbf{P}}_{\mathcal{N}_0} \mathbf{e}_{\mathrm{T}}}{\sqrt{\left(\mathbf{e}_{\mathrm{R}}^H \hat{\mathbf{P}}_{\mathcal{N},\mathrm{R}} \mathbf{e}_{\mathrm{R}}\right)\left(\mathbf{e}_{\mathrm{T}}^H \hat{\mathbf{P}}_{\mathcal{N},\mathrm{T}} \mathbf{e}_{\mathrm{T}}\right)}} \tag{51a}$$

$$= (1 + \rho_{\mathrm{T}} + \rho_{\mathrm{R}} + \rho_{\mathrm{T}}\rho_{\mathrm{R}})^{-1/2}, \tag{51b}$$

with $\hat{\mathbf{P}}_{\mathcal{N},\mathrm{T}} \triangleq \hat{\mathbf{P}}_{\mathcal{N}}(\mathbf{r} = \mathbf{r}_{\mathrm{T}})$ and $\hat{\mathbf{P}}_{\mathcal{N},\mathrm{R}} \triangleq \hat{\mathbf{P}}_{\mathcal{N}}(\mathbf{r} = \mathbf{r}_{\mathrm{R}})$ being the orthogonal projectors onto transmitter's and receiver's sensed noise subspaces, respectively. By defining $\kappa_{\mathrm{T}} \triangleq \kappa(\mathbf{r} = \mathbf{r}_{\mathrm{T}})$ and $\kappa_{\mathrm{R}} \triangleq \kappa(\mathbf{r} = \mathbf{r}_{\mathrm{R}})$ the dimensions of $\mathcal{E}_{\mathrm{T}} \triangleq \mathcal{E}(\mathbf{r} = \mathbf{r}_{\mathrm{T}})$ and $\mathcal{E}_{\mathrm{R}} \triangleq \mathcal{E}(\mathbf{r} = \mathbf{r}_{\mathrm{R}})$, respectively, $\rho_{\mathrm{T}} = \kappa_{\mathrm{T}}/K_0$ and $\rho_{\mathrm{R}} = \kappa_{\mathrm{R}}/K_0$ stand for the normalized subspace dimension excesses at internal transmitter and receiver, respectively. Notice that the selected waveform as a matched-filter detector response does not distort the received waveform. Actually, as we may observe in (51b), the energy injected in $\mathcal{N}_0$ is preserved, and there is a loss factor due to the differences between noise subspaces. In Fig. 6, we illustrate the miss-match loss introduced in (51b).

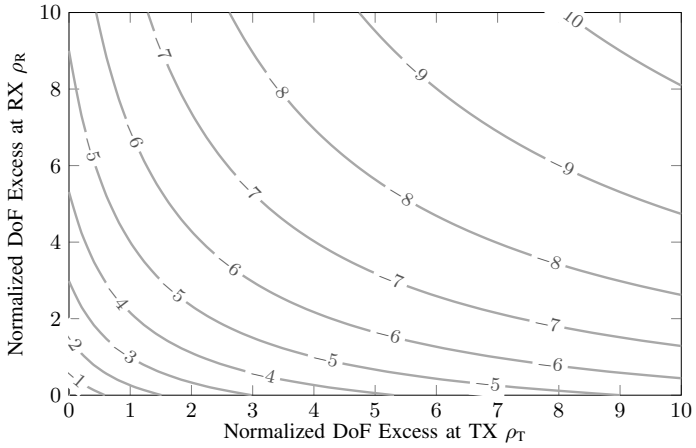

Fig. 6: Contour plot of energy losses [dB] as a function of ρ_{T} and ρ_{R}.

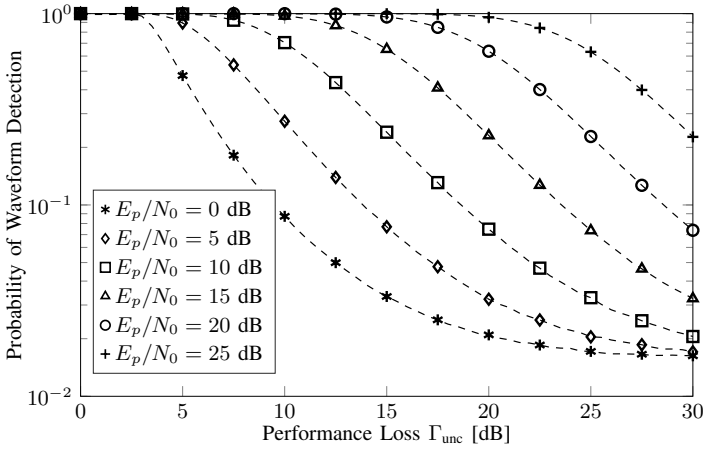

Fig. 7: Probability of Detecting the transmitted waveform versus Γ_{unc}.

Proposition 4 (Robustness to Subspace Uncertainties)**.** *Under the lack of coordination, when the proposed signaling scheme* (17) *is used at both system ends, the information transmitted through the effective noise subspace is not distorted, whereas the subspace excesses ρ_T and ρ_R only introduce an energy loss penalty.*

Even though the interesting observation in Proposition 4, we have previously assumed that the solution is unique at both system ends (cf. Proposition 1). Contrarily, detection uncertainties arises. Therefore, a pulse shaping identification mechanism is further on analyzed.

A. Waveform Detection

Taking into account (46), regardless the noise-subspace basis decomposition presented in (8), these bases can also be decomposed, at each internal-network node as

$$\hat{\mathbf{\Psi}}_{\mathcal{N},\mathrm{T}} = \left[\begin{array}{c:c} \mathbf{\Psi}_{\mathcal{N}}^{(0)} & \mathbf{\Delta}_{\mathrm{T}} \end{array} \right], \tag{52a}$$

$$\hat{\mathbf{\Psi}}_{\mathcal{N},\mathrm{R}} = \left[\begin{array}{c:c} \mathbf{\Psi}_{\mathcal{N}}^{(0)} & \mathbf{\Delta}_{\mathrm{R}} \end{array} \right], \tag{52b}$$

where $\mathcal{N}_0 = \mathrm{span}(\mathbf{\Psi}_{\mathcal{N}}^{(0)})$, and $\mathbf{\Delta}_{\mathrm{T}}$ and $\mathbf{\Delta}_{\mathrm{R}}$ span $\mathcal{E}_{\mathrm{T}}$ and $\mathcal{E}_{\mathrm{R}}$, respectively. From (52a)–(52b) we can immediately see that $K_0 = \mathrm{rank}(\mathbf{\Psi}_{\mathcal{N}}^{(0)})$ and $\kappa(\mathbf{r}) = \mathrm{rank}[\mathbf{\Delta}(\mathbf{r})]$, for $\mathbf{r} = \{\mathbf{r}_{\mathrm{T}}, \mathbf{r}_{\mathrm{R}}\}$.

When the solution is unique, according to Proposition 1, at both system ends, internal nodes are *self-synchronized*. Otherwise, in the worst case, each internal-network user designs a set of N waveforms, namely a *waveform-book*, thusly

$$\mathcal{W}_{\mathrm{T}} = \{\hat{\boldsymbol{\varphi}}_{1,\mathrm{T}}, \ldots, \hat{\boldsymbol{\varphi}}_{N,\mathrm{T}}\} \in \hat{\mathcal{N}}_{\mathrm{T}}, \tag{53a}$$

$$\mathcal{W}_{\mathrm{R}} = \{\hat{\boldsymbol{\varphi}}_{1,\mathrm{R}}, \ldots, \hat{\boldsymbol{\varphi}}_{N,\mathrm{R}}\} \in \hat{\mathcal{N}}_{\mathrm{R}}, \tag{53b}$$

which corresponds to the N columns of orthogonal projectors onto noise subspaces $\hat{\mathcal{N}}_{\mathrm{T}}$ and $\hat{\mathcal{N}}_{\mathrm{R}}$, respectively. Given the ambiguity, internal transmitting node will arbitrarily select one element from $\mathcal{W}_{\mathrm{T}}$, with probability $\frac{1}{N}$. Therefore, in view of Proposition 4, internal receiver should select one shaping filter from $\mathcal{W}_{\mathrm{R}}$ such that the matched-filter loss in (51b) is minimized. Taking into account the mean-square error as a design criterion, the signaling pattern selected by internal-network receiving node obeys

$$\hat{\iota} = \underset{\iota \in \{1,\ldots,N\}}{\arg\max}\ \mathbb{E}\left\{\mathbf{p}(\iota)^H \mathbf{R}_{xx}^{-1} \mathbf{p}(\iota)\right\}. \tag{54}$$

where $\mathbf{p}(\iota) = \mathbb{E}\{\mathbf{x}(n)\hat{\varphi}_{\iota,\mathrm{R}}^*(n)\}$ is the cross-correlation between receiver's input signal $\mathbf{x}(n)$ and the ι-th element from $\mathcal{W}_{\mathrm{R}}$, and $\mathbf{R}_{xx}$ is the input signal autocorrelation matrix. In other words, the receiver's shaping which presents the highest *spectral coherence* with the input signal has to be selected. In Fig. 8 we have depicted one realization of the instantaneous cross-correlation between the waveform arbitrarily selected by internal transmitter and all elements of $\mathcal{W}_{\mathrm{R}}$, for different pulse energy-to-noise ratio E_p/N_0. Note that the detectability is critically affected by subspace uncertainties, specially in low-$\frac{E_p}{N_0}$ scenarios. Although generally $\hat{\mathcal{N}}_{\mathrm{T}} \neq \hat{\mathcal{N}}_{\mathrm{R}}$, detectability is only compromised when subspace uncertainties are meaningful with respect to the uncertainty-free SNR at the receiver.

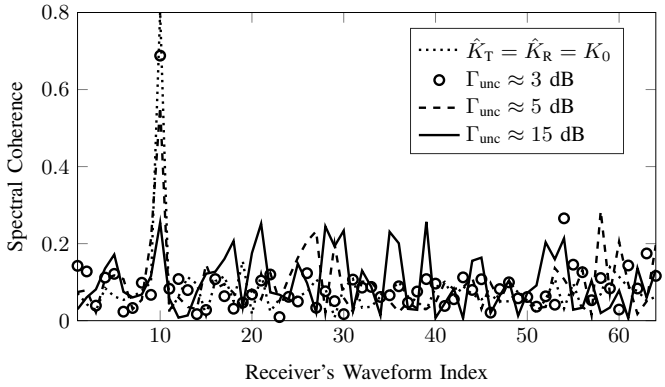

(a) $E_p/N_0 = 10$ dB

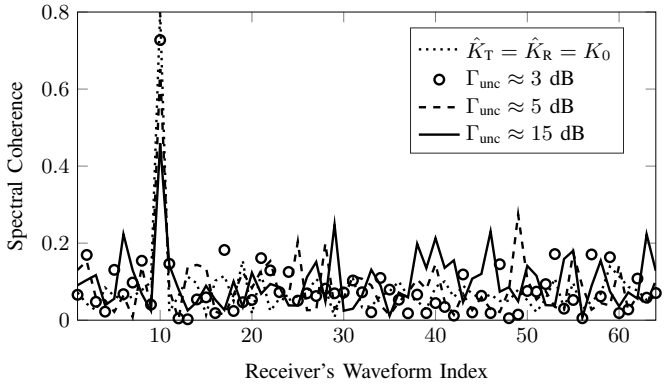

(b) $E_p/N_0 = 30$ dB

Fig. 8: Instantaneous spectral coherence between received signal and all elements of $\mathcal{W}_{\mathrm{R}}$, when the column $n = 10$ from $\mathcal{W}_{\mathrm{T}}$ has been selected.

B. Effects of Uncertainties on Detection Performance

Recalling Proposition 4, information transmitted through $\mathcal{N}_0$ will be detected by internal receiving node. Yet, according to Fig. 5, note that internal transmitter will inject energy to a $\hat{K}_{\mathrm{T}}$-dimensional subspace, whereas internal receiver is detecting on a $\hat{K}_{\mathrm{R}}$-dimensional subspace. Since, in general, $\{\hat{K}_{\mathrm{T}}, \hat{K}_{\mathrm{R}}\} > K_0$, detection performance is worsened by noise enhancement, energy loss and interferences from the wireless environment.

Let X, I and W denote the signal transmitted by an internal-network user, the inter-system interference and a complex additive noise, distributed as $\mathcal{CN}(0, N_0)$, per DoF. Thus, the signal

at ν-th internal receiver's sensed dimension, for $\nu \in \{1, \ldots, \hat{K}_{\mathrm{R}}\}$, can be written as

$$Y_\nu = \begin{cases} X + W & \text{if } \nu \in \mathcal{N}_0 \\ W + I & \text{if } \nu \in \mathcal{P}(\mathcal{E}_{\mathrm{R}}; \epsilon_{\mathrm{R}}) \\ W & \text{if } \nu \in \mathcal{P}(\mathcal{E}_{\mathrm{R}}; \kappa_{\mathrm{R}} - \epsilon_{\mathrm{R}}) \end{cases} \tag{55}$$

where $\mathcal{P}(\mathcal{E}_{\mathrm{R}}; \epsilon_{\mathrm{R}})$ is an ϵ_{R}-dimensional portion of $\mathcal{E}_{\mathrm{R}}$ encompassing those occupied DoF erroneously sensed as available due to sensing errors, and $\mathcal{P}(\mathcal{E}_{\mathrm{R}}; \kappa_{\mathrm{R}} - \epsilon_{\mathrm{R}})$ is a $(\kappa_{\mathrm{R}} - \epsilon_{\mathrm{R}})$-dimensional portion of $\mathcal{E}_{\mathrm{R}}$ including those occupied DoF sensed as available due to monitoring conditions and those available ones sensed as occupied due to false alarm. Thus, by letting G, S_{T} and N_0 be the channel gain, the transmitted power and the one-sided noise spectral density, the SNR at the receiver is given by

$$\mathrm{SNR}_{\mathrm{R}} = \frac{G^2 \cdot K_0 \cdot S_{\mathrm{T}} / \hat{K}_{\mathrm{T}}}{N_0 \hat{K}_{\mathrm{R}} + \sum\limits_{\nu \in \mathcal{P}(\mathcal{E}_{\mathrm{R}}; \epsilon_{\mathrm{R}})} \mathbb{E}\{|I_\nu|^2\}} \tag{56}$$

$$= \underbrace{\frac{\left(1 - \frac{\rho_{\mathrm{T}}}{1+\rho_{\mathrm{T}}}\right)}{(1 + \rho_{\mathrm{R}}) + \overline{\mathrm{inr}} \frac{\epsilon_{\mathrm{R}}}{K_0}}}_{\triangleq\, \Gamma_{\text{unc}}^{-1}} \gamma_{\text{no-unc}}, \tag{57}$$

where $\gamma_{\text{no-unc}} \triangleq G^2 S_{\mathrm{T}} / (K_0 N_0)$ is the uncertainty-free SNR, $\overline{\mathrm{inr}}$ is the average interference-to-noise ratio (INR) per DoF and Γ_{unc} is a performance loss. Hence, the detection performance (which depends on $\mathrm{SNR}_{\mathrm{R}}$) degrades with sensing uncertainties as illustrated in Fig. 7 through the probability of detecting the transmitted waveform (averaged over 10^8 trials).

VII. Effective Noise Subspace Identification

As discussed in Sec. VI, internal-network receiver is generally detecting on a subspace larger than $\mathcal{N}_0$. Furthermore, depending on the selected bases, waveform detection ambiguities may be also present. It is clear that waveform detection will improve, regardless solution ambiguities, if internal receiver adapt its orthogonal projector such that (ideally) only DoF belonging to $\mathcal{N}_0$ are observed. Therefore, recalling Theorem 1 and letting $\boldsymbol{\alpha} = \{0, 1\}^N$ be a sparse vector with only one non-null element, received signal can be estimated as

$$\hat{\mathbf{y}} = \tilde{\mathbf{P}}_{\mathcal{N},\mathrm{R}} \boldsymbol{\alpha}, \tag{58}$$

where $\tilde{\mathbf{P}}_{\mathcal{N},\mathrm{R}}$ is a *modified* orthogonal projector such that

$$\tilde{\mathbf{P}}_{\mathcal{N},\mathrm{R}} = \sum_{n=1}^{\hat{K}_{\mathrm{R}}} \lambda_n \mathbf{P}_n^{(\mathrm{R})}, \tag{59}$$

being $\mathbf{P}_n^{(\mathrm{R})}$ a rank-one orthogonal projector onto the n-the dimension of $\hat{\mathcal{N}}_{\mathrm{R}}$, and $\lambda_n = \{0, 1\}$ is a selection parameter indicating if the n-th dimension belongs to the effective noise subspace or not. By encompassing all λ_n in $\boldsymbol{\lambda}$, and defining $\mathbf{P} = [\mathbf{P}_1, \cdots, \mathbf{P}_{\hat{K}_{\mathrm{R}}}]$, the design of $\boldsymbol{\alpha}$ in (58) and $\boldsymbol{\lambda}$ in (59) can be jointly addressed as

$$\hat{\boldsymbol{\beta}} = \arg\min_{\boldsymbol{\beta}} \ \|\boldsymbol{\beta}\|_1 \ \text{s.t.} \ \mathbf{y} = \mathbf{P}\boldsymbol{\beta}, \tag{60}$$

with $\boldsymbol{\beta} = \boldsymbol{\lambda} \otimes \boldsymbol{\alpha}$. It is worth noting that basis pursuit problem derived in (60) is sensitive to noise, specially in low-SNR regimes. Thus, to address the latter, we let internal receiving node to capture Q observations from internal transmitter. By stacking them in an NQ-length column vector $\tilde{\mathbf{y}} = [\mathbf{y}_1^T \ \cdots \ \mathbf{y}_Q^T]^T$, and defining $\boldsymbol{\Phi}^T = [\mathbf{P} \ \cdots \ \mathbf{P}]$, the *extended* detection problem is cast as

$$\hat{\boldsymbol{\beta}} = \arg\min_{\boldsymbol{\beta}} \ \|\boldsymbol{\beta}\|_1 \ \text{s.t.} \ \|\tilde{\mathbf{y}} - \boldsymbol{\Phi}\boldsymbol{\beta}\|_2^2 \leq \epsilon^2. \tag{61}$$

Finally, note that for large Q, solving (61) becomes computationally unfeasible. Yet, (61) is equivalent to

$$\hat{\boldsymbol{\beta}} = \arg\min_{\boldsymbol{\beta}} \ \|\boldsymbol{\beta}\|_1 \ \text{s.t.} \ \sum_{q=1}^{Q} \|\mathbf{y}_q - \mathbf{P}\boldsymbol{\beta}\|_2^2 \leq \epsilon^2, \tag{62}$$

i.e. solving the full stacked problem in (62) is identical to find the sparsest $\boldsymbol{\beta}$ that minimizes the *cumulative* least-squares error of each N-length sub-block $\mathbf{y}_q$, leading to a more computationally efficient problem feasible to be solved online.

VIII. Distributed Subspace Concurrence

According to the procedure presented in the previous Section, internal-network receiver is able to estimate the effective noise subspace $\mathcal{N}_0$. Recalling Γ_{unc} in (57), detection performance might considerably improve thanks to (62), i.e.

$$\Gamma_{\text{unc}}^{-1} \to 1 - (1 + \rho_{\mathrm{T}})^{-1} \rho_{\mathrm{T}}. \tag{63}$$

Even though the probability of waveform detection rapidly grows as Γ_{unc} vanishes, internal-network transmitter is still using a subspace larger than $\mathcal{N}_0$. Therefore, opportunistic transmission may be energy inefficient and provide inter-system interference to external network. Further on, we address how internal-network transmitter can identify $\mathcal{N}_0$.

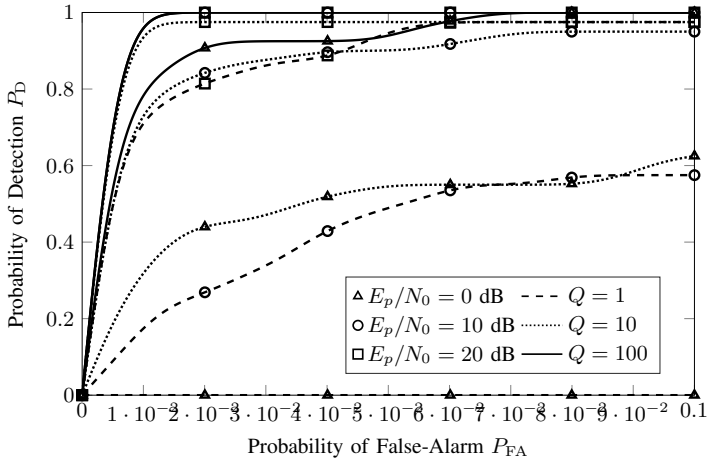

Fig. 9: ROC for $E_p/N_0 = \{0, 10, 20\}$ dB and different block-length $Q = \{1, 10, 100\}$ averaged over 10^4 independent realizations.

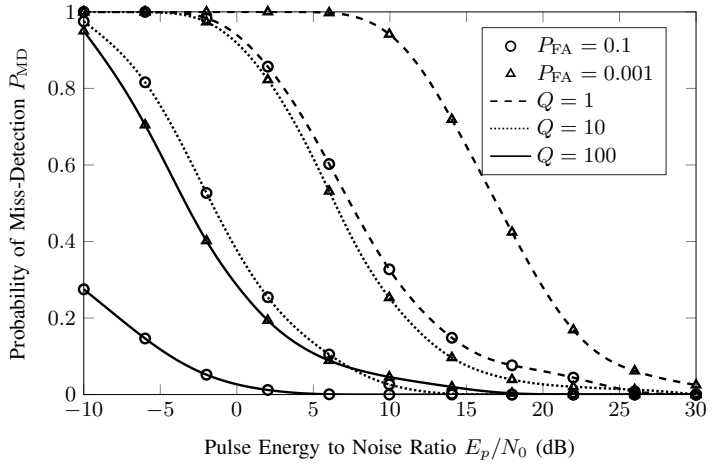

Fig. 10: Probability of Miss-Detection versus E_p/N_0 for different CFAR and block-length $Q = \{1, 10, 100\}$ averaged over 10^4 independent realizations.

A. Noncooperative Subspace Concurrence

Let us assume that internal-network receiver has already performed (62). Hence, it further on uses the shaping filter $\tilde{\boldsymbol{\varphi}}_{\mathrm{R}} = \mathbf{P}\hat{\boldsymbol{\beta}}$ as matched and shaping filters. Since time division duplex (TDD) is the operating mode usually considered in uncoordinated networks, opportunistic transmitter may also try to estimate the effective noise subspace $\mathcal{N}_0$.

To that end, internal transmitter should follow the same procedure performed by internal receiver. Recall how receiver estimates transmitter's waveform (58). To select which DoF belongs

to $\mathcal{N}_0$, the problem is analogous to (58), but using

$$\tilde{\mathbf{P}}_{\mathcal{N},\mathrm{T}} = \sum_{i=1}^{\hat{K}_\mathrm{T}} \pi_i \mathbf{P}_i^{(\mathrm{T})} \tag{64}$$

instead of $\tilde{\mathbf{P}}_{\mathcal{N},\mathrm{R}}$. Notice that $\mathbf{P}_i^{(\mathrm{T})}$ is a rank-one orthogonal projector onto a transmitters's noise subspace singleton and π_i plays the role of λ_i, Thus, recalling the ideas presented in Sec. VII, the agreement problem can be finally cast as in (62).

As numerically reported in Sec. IX, this noncooperative concurrence scheme presents a very good performance under appropriate working conditions. However, whether it is no possible to operate in these regimes, internal-network users will iteratively reduce their noise subspaces until achieving the intersection $\mathcal{N}_0$. Yet, its convergence depends on the operating conditions and opportunistic channel state. In Sec. VIII-B, we introduce a cooperative approach whereby receiver informs transmitter about the estimated $\mathcal{N}_0$.

B. Cooperative Subspace Concurrence

Recent works in the literature highlight the positive impact of cooperation in terms of spectrum sensing [52], security [53], and scheduling [54]. Accordingly, we further on explore the cooperative approach in our problem of subspace concurrence.

First, observe that vector $\boldsymbol{\beta} \in \{0,1\}^{N\hat{K}_\mathrm{R}}$ in (60) can be written as a (sparse) $\hat{K}_\mathrm{R} \times N$ matrix $\mathbf{B}$. Because only one column of the orthogonal projector will be selected by (62), the ij-th entry of $\mathbf{B}$ is given by

$$[\mathbf{B}]_{ij} = \begin{cases} \hat{\lambda}_i & \text{if } j\text{-th column of } \tilde{\mathbf{P}}_{\mathcal{N},\mathrm{R}} \text{ is selected} \\ 0 & \text{otherwise} \end{cases} . \tag{65}$$

Hence, internal-network receiving node can estimate the dimension of the estimated effective noise subspace as

$$\dim[\hat{\mathcal{N}}_0] = \hat{K}_0 = \|\hat{\boldsymbol{\lambda}}\|_0 = \|\hat{\boldsymbol{\beta}}\|_0 \tag{66}$$

Therefore, by using (66) and $\tilde{\boldsymbol{\varphi}}_\mathrm{R} = \mathbf{P}\hat{\boldsymbol{\beta}}$, internal receiver can construct a *feedback message* $\mathbf{f}$ such that

$$\mathbf{f} = \left[\hat{K}_0,\ \tilde{\boldsymbol{\varphi}}_\mathrm{R}^T\right]^T \in \mathbb{C}^{N+1}. \tag{67}$$

Even though the concurrence problem proposed in Sec. VIII-A can be seen as a *sparse recovery* problem without information on the required sparsity, internal-network transmitter is now able to exploit the side information encompassed in (67) to improve the estimation of $\mathcal{N}_0$. By letting

$\boldsymbol{\gamma}$ play the role of $\boldsymbol{\beta}$ at transmitter side, a more informative problem can be addressed. In this sense, we propose the following optimization problem:

$$\min_{\boldsymbol{\gamma}} \ \|\mathbf{P}\boldsymbol{\gamma} - \tilde{\boldsymbol{\varphi}}_{\mathrm{R}}\|_2^2 \text{ s.t. } \|\boldsymbol{\gamma}\|_0 \leq \tilde{K}_0, \tag{68}$$

where $\tilde{\boldsymbol{\varphi}}_{\mathrm{R}}$ and $\tilde{K}_0$ are fed-back by receiver through (67). Unfortunately, the sparsity constraint in (68) is an NP-hard (i.e. non-convex) problem. Classically, in the context of compressed sensing and sparse recovery, this sparsity constraint is relaxed. Hence the problem in (68) can be cast as the LASSO or basis pursuit denoising as

$$\min_{\boldsymbol{\gamma}} \ \|\mathbf{P}\boldsymbol{\gamma} - \tilde{\boldsymbol{\varphi}}_{\mathrm{R}}\|_2^2 \text{ s.t. } \|\boldsymbol{\gamma}\|_1 \leq \tilde{K}_0. \tag{69}$$

In general, when (69) is addressed, the *exact* recovery cannot be guaranteed in general. Yet, as stated in Lemma 1 (proved in [2] and in Appendix B), (68) and (69) can be equivalent, and hence the sparse vector $\boldsymbol{\gamma}$ can be recovered.

Lemma 1. *Optimization problem in* (69) *is equivalent to that in* (68)*, under the Restricted Isometry Property (RIP) [55], when the solution is not unique according to Proposition 1.*

IX. Simulation Analysis

In this Section, we report a numerical assessment of the algorithms presented in Sec. VII and VIII. To that end, we consider a heterogeneous network composed of an arbitrary number of users operating in a 64-dimensional subspace. For the sake of simplicity, we assume that both internal-network transmitter and receiver observe the same wireless environment. Further, we consider that both system ends detect a DoF occupation of $3/8$. Hence, the available DoF for opportunistic communication are encompassed in a 40-dimensional subspace. Finally, we assume a normalized DoF excess at both system ends of $\rho_{\mathrm{T}} = \rho_{\mathrm{R}} = 30\%$. A possible scenario with the aforementioned features is that where each internal-network user observes the same wireless environment and the sensing mechanisms has almost negligible false-alarm probabilities. Nevertheless, both opportunistic nodes have detected 52 available DoF, with 12 out of 52 are erroneously sensed as available. Recalling the discussion in Sec. VI, albeit the matched-filter loss is very small, the waveform detection probability can be severely reduced specially if these excess provides inter-system interference to internal-network receiver. Furthermore, since the excess at transmitting side may yield inter-system interferences to external network, subspace concurrence is of paramount necessity to avoid them.

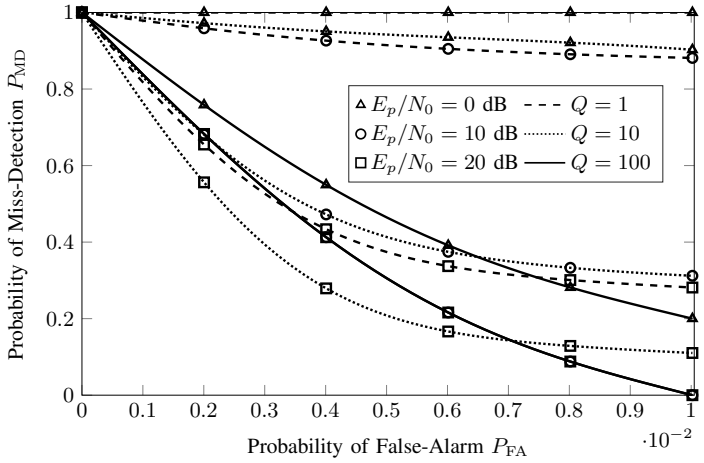

Fig. 11: Complementary ROC of noncooperative scheme for different E_p/N_0 and block-length Q averaged over 10^4 independent trials.

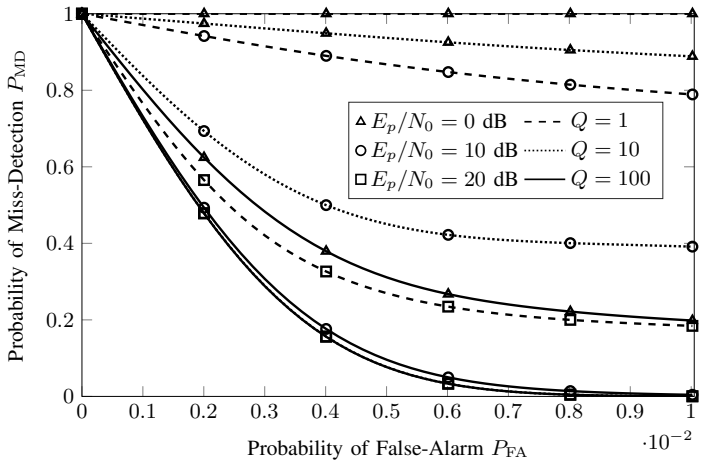

Fig. 12: Complementary ROC of cooperative scheme for different E_p/N_0 and block-length Q averaged over 10^4 independent trials.

A. Estimation of $\mathcal{N}_0$ at Internal-Network Receiver

First of all, we analyze the performance of the effective noise subspace identification algorithm proposed in Sec. VII. As performance metrics, we define the probability of correct detection P_{D} as the probability of detecting as active a DoF belonging to $\mathcal{N}_0$. Likewise, we define the miss-detection probability as $P_{\mathrm{MD}} \triangleq 1 - P_{\mathrm{D}}$. In Fig. 9 we have depicted the Receiver Operating Characteristics (ROC) of (62) for different E_p/N_0 and block-length Q. By defining the false-alarm probability P_{FA} as the probability of selecting a DoF not belonging to $\mathcal{N}_0$ and $\mathcal{Q}(\cdot)$ the tail probability of a Gaussian distribution, we have considered the following decision threshold $\gamma = \sqrt{\sigma_{\mathrm{R}}^2/Q}\mathcal{Q}^{-1}(P_{\mathrm{FA}})$ in order to guarantee the optimality in the Neyman-Pearson sense. The

effects of E_p/N_0 in P_{MD} for fixed P_{FA} are illustrated in Fig. 10. From both figures we may conclude that proposed scheme presents a good performance even for small P_{FA} when operating conditions (E_p/N_0 and Q) are good enough.

B. Estimation of $\mathcal{N}_0$ at Internal-Network Transmitter

It is worth noticing that the performance of $\mathcal{N}_0$ estimation at transmitter side substantially depends on the performance achieved at receiving side. For the sake of simplicity, we will further on assume that opportunistic receiver has been able to detect the whole $\mathcal{N}_0$. Under this assumption, we assess both the noncooperative and cooperative schemes presented in Sec. VIII. Notice that noncooperative one is exactly the same as in the previous subsection. We can observe in Fig. 11 and 12 that cooperative scheme achieves the same performance than noncooperative one in terms of P_{MD} for smaller P_{FA}. In Fig. 13 we illustrate the performance of both concurrence schemes in terms of the average number of DoF belonging to $\mathcal{N}_0$ correctly identified as a function of P_{FA} for different E_p/N_0. Note that cooperative scheme presents a higher identification performance than noncooperative one even for small P_{FA}.

C. Subspace Concurrence Assessment

Under the operating conditions of internal-network receiver assumed in the previous subsection, we analyze the capacity of both concurrence schemes to achieve subspace consensus. In order to measure the similarity between sensed effective noise subspaces at both system ends, we have considered the *extrinsic distance* between subspaces or *chordal distance*:

$$d^2_{\mathrm{chordal}} = \frac{1}{2}\left\|\tilde{\mathbf{P}}_{\mathcal{N},\mathrm{T}} - \tilde{\mathbf{P}}_{\mathcal{N},\mathrm{R}}\right\|^2_{\mathrm{F}}, \tag{70}$$

where $\tilde{\mathbf{P}}_{\mathcal{N},\mathrm{T}}$ and $\tilde{\mathbf{P}}_{\mathcal{N},\mathrm{R}}$ are the modified projectors onto the estimated effective noise subspace at transmitting and receiving sides, respectively. As depicted in Fig. 14, for very small P_{FA}, both agreement schemes are able to obtain a very acceptable subspace consensus in terms of chordal distance.

X. Conclusions

In this work, we proposed a novel distributed design of context-aware invariant signaling patterns for opportunistic communications. By addressing the problem as a total least-squares

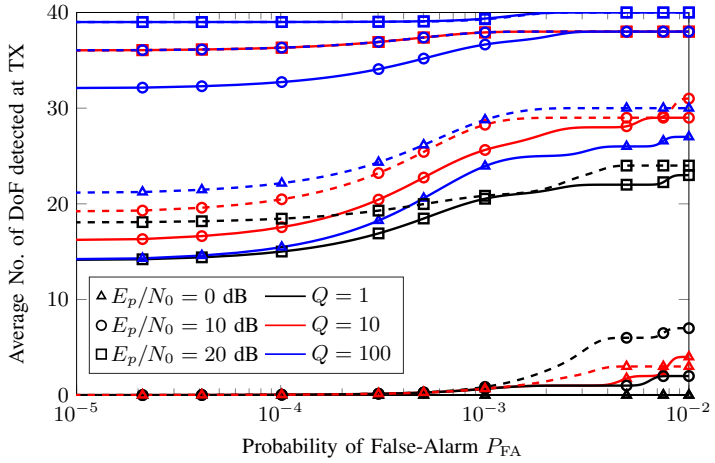

Fig. 13: Average number of identified DoF at TX versus P_{FA}. Solid and dashed lines refer to noncooperative and cooperative concurrence schemes.

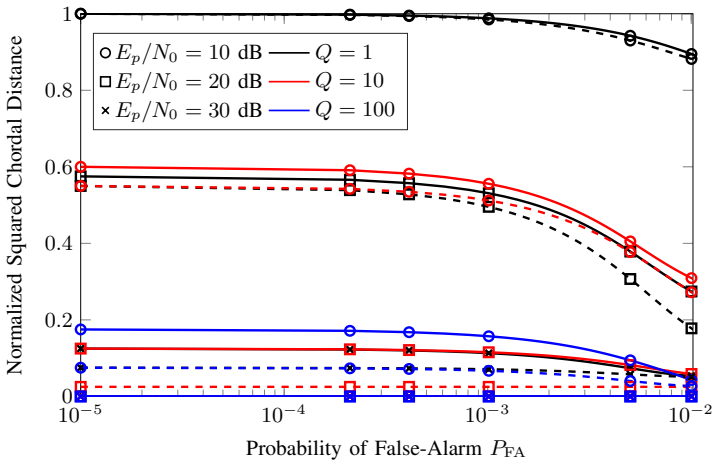

Fig. 14: Normalized (70) versus P_{FA} with (dashed) and without (solid) cooperation for different E_p/N_0 and block-length Q averaged over 10^4 trials.

optimization, we saw that the proposed solution is robust in front sensing uncertainties, guaranteeing minimum inter-system interference. Furthermore, due to the equivalence with minimum norm, invariance to noise-subspace rotations is also exhibited. Nevertheless, given the locality of the presented approach, end-to-end subspace uncertainties may yield both inter-system interference and a performance loss. To overcome the latter, we analyzed the distributed subspace agreement problem with and without side information.

APPENDIX A
PROOF OF PROPOSITION 3

Let $\boldsymbol{\phi} = \hat{\boldsymbol{\Psi}}_{\mathcal{N}}^{H}\hat{\boldsymbol{\varphi}}_n$ contain the $\hat{K}$ relevant components of $\hat{\boldsymbol{\varphi}}_n$. The power distribution can be then calculated as

$$\mathbf{R}_{\phi\phi} = \boldsymbol{\phi}\boldsymbol{\phi}^{H} = \hat{\boldsymbol{\Psi}}_{\mathcal{N}}^{H}\hat{\boldsymbol{\varphi}}_n\hat{\boldsymbol{\varphi}}_n^{H}\hat{\boldsymbol{\Psi}}_{\mathcal{N}}^{H} = \mathbf{I}_{\hat{K}}.$$

Hence, the power is equally distributed among $\hat{K}$ DoF sensed as available. As follows from (40), the power injected to the ξ incorrectly sensed as available DoF is minimum. Therefore, the inter-system interference per DoF must be minimum.

APPENDIX B
PROOF OF LEMMA 1

A *measurement matrix* $\boldsymbol{\Omega}$ satisfies the RIP for all n-sparse vectors $\boldsymbol{\upsilon}$ with parameters (n, ε) whether

$$(1-\varepsilon)\|\boldsymbol{\upsilon}\|_2 \leq \|\boldsymbol{\Omega}\boldsymbol{\upsilon}\|_2 \leq (1+\varepsilon)\|\boldsymbol{\upsilon}\|_2,\ \forall\varepsilon \in (0,1) \tag{71}$$

Recall that, in our problem, $\boldsymbol{\upsilon} = \boldsymbol{\gamma} \in \{0,1\}^{NK_{\mathrm{T}}}$ and $\boldsymbol{\Omega} = \mathbf{P} \in \mathbb{C}^{N\times NK_{\mathrm{T}}}$. Regarding to the left-hand side of (71), it is worth noting that

$$\|\boldsymbol{\gamma}\|_2 = \sqrt{\boldsymbol{\gamma}^{H}\boldsymbol{\gamma}} = \sqrt{\hat{K}_0^{(\mathrm{T})}}. \tag{72}$$

Now, recall that $\boldsymbol{\gamma} = \boldsymbol{\pi} \otimes \boldsymbol{\alpha}$, where $\boldsymbol{\pi}$ selects the active DoF and $\boldsymbol{\alpha}$ chooses a column from $\tilde{\mathbf{P}}_{\mathcal{N},\mathrm{T}}$. By taking a look at the central part of (71), adapted to our problem, we have that

$$\|\mathbf{P}\boldsymbol{\gamma}\|_2 = \sqrt{\boldsymbol{\gamma}^{H}\mathbf{P}^{H}\mathbf{P}\boldsymbol{\gamma}} \tag{73}$$

$$= \left(\begin{bmatrix} \pi_1\boldsymbol{\alpha}^{T} \cdots \pi_{\hat{K}_{\mathrm{T}}}\boldsymbol{\alpha}^{T} \end{bmatrix} \begin{bmatrix} \mathbf{P}_1 & \mathbf{0} & \cdots & \mathbf{0} \\ \mathbf{0} & \mathbf{P}_2 & \cdots & \vdots \\ \vdots & \mathbf{0} & \ddots & \mathbf{0} \\ \mathbf{0} & \mathbf{0} & \cdots & \mathbf{P}_{\hat{K}_{\mathrm{T}}} \end{bmatrix} \begin{bmatrix} \pi_1\boldsymbol{\alpha} \\ \vdots \\ \pi_{\hat{K}_{\mathrm{T}}}\boldsymbol{\alpha} \end{bmatrix} \right)^{-1/2} \tag{74}$$

$$= \sqrt{\sum_{i=1}^{\hat{K}_{\mathrm{T}}} \pi_i^2 \left[\mathbf{P}_i\right]_{\hat{\imath},\hat{\imath}}}. \tag{75}$$

Notice that (75) is equal to $\sqrt{\hat{K}_0^{(\mathrm{T})}}$ when the diagonal entries of each $\mathbf{P}_i$ are ones. By noting that this happens when rank-one projectors are obtained from canonical basis or elements of bases are complex exponentials (which will asymptotically occur), RIP is satisfied in these two

cases for all possible ε. Otherwise, the second inequality in (71) is always satisfied, but nothing can be said about the first one.

REFERENCES

[1] J. Borràs and G. Vázquez, "Decentralized shaping for pilot generation and detection in opportunistic communications," in *2019 IEEE Int. Conf. Commun. (ICC)*, May 2019, pp. 1–5.

[2] J. Borràs and G. Vázquez, "Distributed feedback-aided subspace concurrent opportunistic communications," in *2019 IEEE 20th Int. Workshop Signal Process. Adv. Wireless Commun. (SPAWC)*, Jul 2019, pp. 1–5.

[3] L. Lu, G. Y. Li, A. Maaref, and R. Yao, "Opportunistic transmission exploiting frequency- and spatial-domain degrees of freedom," *IEEE Wireless Commun.*, vol. 21, no. 2, pp. 91–97, Apr 2014.

[4] P. Viswanath, D. N. C. Tse, and R. Laroia, "Opportunistic beamforming using dumb antennas," *IEEE Trans. Inf. Theory*, vol. 48, no. 6, pp. 1277–1294, Jun 2002.

[5] S. Haykin, "Cognitive radio: brain-empowered wireless communications," *IEEE J. Sel. Areas Commun.*, vol. 23, no. 2, pp. 201–220, Feb 2005.

[6] A. Goldsmith, S. A. Jafar, I. Maric, and S. Srinivasa, "Breaking spectrum gridlock with cognitive radios: an information theoretic perspective," *Proc. IEEE*, vol. 97, no. 5, pp. 894–914, May 2009.

[7] D. Lopez-Perez, I. Guvenc, G. de la Roche, M. Kountouris, T. Q. S. Quek, and J. Zhang, "Enhanced intercell interference coordination challenges in heterogeneous networks," *IEEE Wireless Commun.*, vol. 18, no. 3, pp. 22–30, Jun 2011.

[8] F. Jameel, Z. Hamid, F. Jabeen, S. Zeadally, and M. A. Javed, "A survey of device-to-device communications: research issues and challenges," *IEEE Commun. Surveys Tut.*, pp. 1–1, 2018.

[9] Q. Zhao and A. Swami, "A survey of dynamic spectrum access: Signal processing and networking perspectives," in *2007 IEEE Int. Conf. Acoust., Speech, Signal Process. - ICASSP '07*, vol. 4, Apr 2007, pp. IV–1349–IV–1352.

[10] E. Axell, G. Leus, E. G. Larsson, and H. V. Poor, "Spectrum sensing for cognitive radio : State-of-the-art and recent advances," *IEEE Signal Process. Mag.*, vol. 29, no. 3, pp. 101–116, May 2012.

[11] H. Yi, H. Hu, Y. Rui, K. Guo, and J. Zhang, "Null space-based precoding scheme for secondary transmission in a cognitive radio MIMO system using second-order statistics," in *2009 IEEE Int. Conf. Commun.*, Jun 2009, pp. 1–5.

[12] L. S. Cardoso, M. Kobayashi, F. R. P. Cavalcanti, and M. Debbah, "Vandermonde-subspace frequency division multiplexing for two-tiered cognitive radio networks," *IEEE Trans. Commun.*, vol. 61, no. 6, pp. 2212–2220, Jun 2013.

[13] R. Yao, Y. Liu, L. Lu, G. Y. Li, and A. Maaref, "Cooperative capacity-achieving precoding design for multi-user VFDM transmission," in *2014 IEEE Global Conf. Signal and Inf. Process. (GlobalSIP)*, Dec 2014, pp. 1296–1300.

[14] R. Yao, Y. Liu, L. Lu, G. Y. Li, and A. Maaref, "Cooperative precoding for cognitive transmission in two-tier networks," *IEEE Trans. Commun.*, vol. 64, no. 4, pp. 1423–1436, Apr 2016.

[15] J. Font-Segura, G. Vazquez, and J. Riba, "Exploiting cognitive cyclostationary noise subspace for noncognitive spectrum sensing," in *2013 IEEE 14th Int. Workshop Signal Process. Adv. Wireless Commun. (SPAWC)*, Jun 2013, pp. 110–114.

[16] R. Zhang and Y. C. Liang, "Exploiting multi-antennas for opportunistic spectrum sharing in cognitive radio networks," *IEEE J. Sel. Topics Signal Process.*, vol. 2, no. 1, pp. 88–102, Feb 2008.

[17] Y. Zhang, E. Dall'Anese, and G. B. Giannakis, "Distributed robust beamforming for MIMO cognitive networks," in *2012 IEEE Int. Conf. Acoust., Speech, Signal Process. (ICASSP)*, Mar 2012, pp. 2953–2956.

[18] Y. Zhang, E. Dall'Anese, and G. B. Giannakis, "Distributed optimal beamformers for cognitive radios robust to channel uncertainties," *IEEE Trans. Signal Process.*, vol. 60, no. 12, pp. 6495–6508, Dec 2012.

[19] G. Zheng, K. K. Wong, and B. Ottersten, "Robust cognitive beamforming with bounded channel uncertainties," *IEEE Trans. Signal Process.*, vol. 57, no. 12, pp. 4871–4881, Dec 2009.

[20] M. H. Al-Ali and K. C. Ho, "Transmit precoding in underlay MIMO cognitive radio with unavailable or imperfect knowledge of primary interference channel," *IEEE Trans. Wireless Commun.*, vol. 15, no. 8, pp. 5143–5155, Aug 2016.

[21] M. H. Al-Ali and D. K. C. Ho, "Precoding for MIMO channels in cognitive radio networks with CSI uncertainties and for MIMO compound capacity," *IEEE Trans. Signal Process.*, vol. 65, no. 15, pp. 3976–3989, Aug 2017.

[22] L. Lu, G. Y. Li, and A. Maaref, "Spatial-frequency signal alignment for opportunistic transmission," *IEEE Trans. Signal Process.*, vol. 62, no. 6, pp. 1561–1575, Mar 2014.

[23] M. Bica, K. Huang, U. Mitra, and V. Koivunen, "Opportunistic radar waveform design in joint radar and cellular communication systems," in *2015 IEEE Global Commun. Conf. (GLOBECOM)*, Dec 2015, pp. 1–7.

[24] W. Hedhly, O. Amin, and M. Alouini, "Interweave cognitive radio with improper Gaussian signaling," in *2017 IEEE Global Commun. Conf. (GLOBECOM)*, Dec 2017, pp. 1–6.

[25] F. Zhou, Y. Wu, Y. Liang, Z. Li, Y. Wang, and K. Wong, "State of the art, taxonomy, and open issues on cognitive radio networks with NOMA," *IEEE Wireless Commun.*, vol. 25, no. 2, pp. 100–108, Apr 2018.

[26] R. G. Gallager, *Information Theory and Reliable Communications*. John Wiley & Sons, 1968.

[27] D. Tse and P. Viswanath, *Fundamentals of Wireless Communication*. Cambridge University Press, 2005.

[28] A. Ali and W. Hamouda, "Advances on spectrum sensing for cognitive radio networks: Theory and applications," *IEEE Commun. Surveys Tut.*, vol. 19, no. 2, pp. 1277–1304, Secondquarter 2017.

[29] R. Tandra and A. Sahai, "SNR walls for signal detection," *IEEE J. Sel. Topics Signal Process.*, vol. 2, no. 1, pp. 4–17, Feb 2008.

[30] S. A. Razavi, M. Valkama, and D. Cabric, "Covariance-based OFDM spectrum sensing with sub-nyquist samples," *Signal Process.*, vol. 109, pp. 261 – 268, 2015.

[31] J. Riba, J. Font-Segura, J. Villares, and G. VÃązquez, "Frequency-domain GLR detection of a second-order cyclostationary signal over fading channels," *IEEE Trans. Signal Process.*, vol. 62, no. 8, pp. 1899–1912, Apr 2014.

[32] M. Jin, Y. Li, and H. Ryu, "On the performance of covariance based spectrum sensing for cognitive radio," *IEEE Trans. Signal Process.*, vol. 60, no. 7, pp. 3670–3682, Jul 2012.

[33] B. Farhang-Boroujeny and R. Kempter, "Multicarrier communication techniques for spectrum sensing and communication in cognitive radios," *IEEE Commun. Mag.*, vol. 46, no. 4, pp. 80–85, Apr 2008.

[34] K. Bouallegue, I. Dayoub, M. Gharbi, and K. Hassan, "Blind spectrum sensing using extreme eigenvalues for cognitive radio networks," *IEEE Commun. Lett.*, vol. 22, no. 7, pp. 1386–1389, Jul 2018.

[35] P. Stoica and Y. Selen, "Model-order selection: a review of information criterion rules," *IEEE Signal Process. Mag.*, vol. 21, no. 4, pp. 36–47, Jul 2004.

[36] A. Mariani, A. Giorgetti, and M. Chiani, "Wideband spectrum sensing by model order selection," *IEEE Trans. Wireless Commun.*, vol. 14, no. 12, pp. 6710–6721, Dec 2015.

[37] J. Font-Segura, G. VÃązquez, and J. Riba, "Single and multi-frequency wideband spectrum sensing with side-information," *IET Signal Process.*, vol. 8, no. 8, pp. 831–843, 2014.

[38] K. Cichon, A. Kliks, and H. Bogucka, "Energy-efficient cooperative spectrum sensing: A survey," *IEEE Commun. Surveys Tut.*, vol. 18, no. 3, pp. 1861–1886, thirdquarter 2016.

[39] A. Patel, H. Ram, A. K. Jagannatham, and P. K. Varshney, "Robust cooperative spectrum sensing for MIMO cognitive radio networks under CSI uncertainty," *IEEE Trans. Signal Process.*, vol. 66, no. 1, pp. 18–33, Jan 2018.

[40] J. Tong, M. Jin, Q. Guo, and Y. Li, "Cooperative spectrum sensing: A blind and soft fusion detector," *IEEE Trans. Wireless Commun.*, vol. 17, no. 4, pp. 2726–2737, Apr 2018.

[41] G. Vazquez-Vilar, R. Lopez-Valcarce, and J. Sala, "Multiantenna spectrum sensing exploiting spectral a priori information," *IEEE Trans. Wireless Commun.*, vol. 10, no. 12, pp. 4345–4355, Dec 2011.

[42] C. G. Tsinos and K. Berberidis, "Decentralized adaptive eigenvalue-based spectrum sensing for multiantenna cognitive radio systems," *IEEE Trans. Wireless Commun.*, vol. 14, no. 3, pp. 1703–1715, Mar 2015.

[43] G. H. Golub and C. F. V. Loan, "An analysis of the total least squares problem," *SIAM J. Numerical Anal.*, vol. 17, no. 6, pp. 883–893, 1980.

[44] R. T. Behrens and L. L. Scharf, "Signal processing applications of oblique projection operators," *IEEE Trans. Signal Process.*, vol. 42, no. 6, pp. 1413–1424, Jun 1994.

[45] E. M. Dowling and R. D. DeGroat, "The equivalence of the total least squares and minimum norm methods," *IEEE Trans. Signal Process.*, vol. 39, no. 8, pp. 1891–1892, Aug 1991.

[46] I. Markovsky and S. V. Huffel, "Overview of total least-squares methods," *Signal Process.*, vol. 87, no. 10, pp. 2283–2302, 2007.

[47] R. Kumaresan and D. Tufts, "Estimating the parameters of exponentially damped sinusoids and pole-zero modeling in noise," *IEEE Trans. Acoust., Speech, Signal Process.*, vol. 30, no. 6, pp. 833–840, Dec 1982.

[48] R. Kumaresan and D. W. Tufts, "Estimating the angles of arrival of multiple plane waves," *IEEE Trans. Aerosp. Electron. Syst.*, vol. AES-19, no. 1, pp. 134–139, Jan 1983.

[49] J. Borràs, J. Font-Segura, J. Riba, and G. Vázquez, "Dimension spreading for coherent opportunistic communications," in *2017 51st Asilomar Conf. Signals, Syst. Comput.*, Oct 2017, pp. 1940–1944.

[50] J. Borràs and G. Vázquez, "Uncoordinated space-frequency pilot design for multi-antenna wideband opportunistic communications," in *2018 IEEE 19th Int. Workshop Signal Process. Adv. Wireless Commun. (SPAWC)*, Jun 2018, pp. 1–5.

[51] R. Kumaresan, "On the zeros of the linear prediction-error filter for deterministic signals," *IEEE Trans. Acoust., Speech, Signal Process.*, vol. 31, no. 1, pp. 217–220, Feb 1983.

[52] W. Liang, S. X. Ng, and L. Hanzo, "Cooperative overlay spectrum access in cognitive radio networks," *IEEE Commun. Surveys Tut.*, vol. 19, no. 3, pp. 1924–1944, thirdquarter 2017.

[53] M. Nguyen, N. Nguyen, D. B. Da Costa, H. Nguyen, and R. T. De Sousa, "Secure cooperative half-duplex cognitive radio networks with k -th best relay selection," *IEEE Access*, vol. 5, pp. 6678–6687, 2017.

[54] S. S. Kalamkar, J. P. Jeyaraj, A. Banerjee, and K. Rajawat, "Resource allocation and fairness in wireless powered cooperative cognitive radio networks," *IEEE Trans. Commun.*, vol. 64, no. 8, pp. 3246–3261, Aug 2016.

[55] E. J. Candes and T. Tao, "Decoding by linear programming," *IEEE Trans. Inf. Theory*, vol. 51, no. 12, pp. 4203–4215, Dec 2005.